

Variance-based global sensitivity analysis for multiple scenarios and models with implementation using sparse grid collocation



Heng Dai¹, Ming Ye^{*}

Department of Scientific Computing, Florida State University, Tallahassee, FL 32306, USA

ARTICLE INFO

Article history:

Received 3 February 2015

Received in revised form 14 May 2015

Accepted 15 June 2015

Available online 21 June 2015

This manuscript was handled by Andras Bardossy, Editor-in-Chief, with the assistance of Wolfgang Nowak, Associate Editor

Keywords:

Model uncertainty

Model averaging

Scenario uncertainty

Scenario averaging

Variance decomposition

Sparse grid collocation

SUMMARY

Sensitivity analysis is a vital tool in hydrological modeling to identify influential parameters for inverse modeling and uncertainty analysis, and variance-based global sensitivity analysis has gained popularity. However, the conventional global sensitivity indices are defined with consideration of only parametric uncertainty. Based on a hierarchical structure of parameter, model, and scenario uncertainties and on recently developed techniques of model- and scenario-averaging, this study derives new global sensitivity indices for multiple models and multiple scenarios. To reduce computational cost of variance-based global sensitivity analysis, sparse grid collocation method is used to evaluate the mean and variance terms involved in the variance-based global sensitivity analysis. In a simple synthetic case of groundwater flow and reactive transport, it is demonstrated that the global sensitivity indices vary substantially between the four models and three scenarios. Not considering the model and scenario uncertainties, might result in biased identification of important model parameters. This problem is resolved by using the new indices defined for multiple models and/or multiple scenarios. This is particularly true when the sensitivity indices and model/scenario probabilities vary substantially. The sparse grid collocation method dramatically reduces the computational cost, in comparison with the popular quasi-random sampling method. The new framework of global sensitivity analysis is mathematically general, and can be applied to a wide range of hydrologic and environmental problems.

© 2015 Elsevier B.V. All rights reserved.

1. Introduction

Sensitivity analysis is a vital tool in hydrological modeling to identify influential parameters for inverse modeling and uncertainty analysis. There has been a growing trend of using global sensitivity analysis, which, in comparison with local sensitivity analysis, considers entire ranges of model parameters and takes into account the interactions between different parameters (van Griensven et al., 2006; Herman et al., 2013; Mishra et al., 2009; Nossent et al., 2011; Pan et al., 2011; Saltelli, 2000; Saltelli et al., 2010; Saltelli and Sobol, 1995; Shi et al., 2014; Song et al., 2015; Yang, 2011). Among various global sensitivity analysis methods, variance-based methods (Sobol', 1993; Saltelli et al., 1999) have gained popularity (Massmann and Holzmann, 2012; van Werkhoven et al., 2008; Wagener et al., 2009; Yang, 2011; Zhang et al., 2013a, 2013b). Different from screening methods (e.g., Morris methods, Morris, 1991), the variance-based methods

provide not only ranking of parameter importance but also quantitative sensitivity measures such as global sensitivity indices for different parameters. The quantitative measures have been used recently for model structure diagnosis with respect to model complexity and model structure inadequacy (Rosolem et al., 2012; Gupta et al., 2012). For example, van Werkhoven et al. (2008) used Sobol's variance-based global sensitivity analysis to evaluate whether moderate model complexity is adequate for modeling multiple watersheds. Herman et al. (2013) further extended the global sensitivity analysis to three different models for understanding intermodel differences in dominant model parameters and/or components. These researches have shown promise in revealing contrasting controls across individual models.

This paper presents a new method that uses variance-based global sensitivity analysis beyond individual models but in the model averaging framework. New global sensitivity indices are derived for multiple models to identify influential parameters for not only individual models but also all models on average. This is necessary when model uncertainty exists, because parameter sensitivity varies (sometimes substantially) between models (Herman et al., 2013; Van Werkhoven et al., 2008) and identifying important parameters for a single model may be biased in that the important

^{*} Corresponding author. Tel.: +1 850 644 4587; fax: +1 850 644 0098.

E-mail address: mye@fsu.edu (M. Ye).

¹ Present address: Pacific Northwest National Laboratory, Richland, WA 99352, USA.

parameters identified for a single model may not be important to the processes that the model intend to simulate. The bias in parameter identification can be reduced by the new global sensitivity indices based on model averaging for addressing model uncertainty. Model uncertainty is caused by multiple plausible interpretations of the system of interest based on available data and knowledge. For the hydrological modeling, model uncertainty is often inevitable, because the open and complex hydrologic systems can be conceptually interpreted and mathematically described in multiple ways (Beven, 2002, 2006; Bredehoeft, 2003, 2005; Neuman, 2003). Model averaging is a popular method for addressing and quantifying model uncertainty by evaluating the weighted average of the simulations of alternative models. The weights are measures of model plausibility, and can be estimated using various methods (Foglia et al., 2013; Lu et al., 2013; Tsai and Elshali, 2013; Ye et al. (2010b); Tsai and Li, 2008; Ye et al. (2008a); Meyer et al., 2007; Ajami et al., 2007; Poeter and Anderson, 2005; Ye et al., 2004; Winter and Nychka, 2010; Wohling and Vrugt, 2008). Schoniger et al. (2014) recently reported a comprehensive review and comparison of the methods used to estimate the Bayesian model averaging weights. Since our new sensitivity indices are based on the concept of model averaging (not specifically Bayesian model averaging), the indices can be evaluated by using the weights estimated via any methods. In addition, the weights can be estimated using expert judgments only or using both expert judgment and observations. The former is equivalent to prior weights and the latter to posterior weights, from a Bayesian viewpoint. In this study, only the prior weights are used, since evaluating posterior weights is beyond the scope of this work.

In addition to model uncertainty, the new method of variance-based global sensitivity analysis also considers scenario uncertainty by estimating the new global sensitivity indices for a set of scenarios in a scenario averaging framework. Scenario uncertainty is aleatory and an important source of predictive uncertainty. According to IPCC (2000, p.62), “scenarios are images of the future, or alternative futures. They are neither predictions nor forecasts. Rather, each scenario is one alternative image of how the future might unfold. A set of scenarios assists in the understanding of possible future developments of complex systems.” Following Meyer et al. (2014), a scenario of hydrologic modeling is defined in this paper as a future state or condition assumed for a system, with the emphasis on those aspects of a scenario that affect the system hydrology. Scenario uncertainty here is similar to the input uncertainty used in surface hydrology (e.g., Kavetski et al., 2006; Vrugt et al., 2008; Renard et al., 2010), but with focus on future states and conditions. While it happens often that the same models are used for different scenarios, different models may be needed for different scenarios, when scenario uncertainty affects model formulation. On the other hand, for the same model, its plausibility may vary under different scenarios, because prior probability may change given that the model is conditioned on scenarios, although scenario uncertainty does not affect model calibration. Based on the concept that model uncertainty depends on scenario uncertainty, Draper et al. (1999) developed a scenario- and model-averaging method to first quantify model uncertainty and then scenario uncertainty. Similarly, Meyer et al. (2007, 2014) developed a hierarchical Bayesian framework to quantify parametric, model, and scenario uncertainty. The hierarchical framework was also used by Rojas et al. (2010) for quantifying scenario and model uncertainties for a system with multiple models and scenarios. It is for the first time that the hierarchical framework is used for global sensitivity analysis to define global sensitivity indices with consideration of multiple models and scenarios. Without loss of generality, the numerical example of this study uses the same models for different scenarios.

As discussed above, instead of considering only parametric uncertainty under a single model and a single scenario, our new

variance-based global sensitivity considers the joint effect of parametric, model, and scenario uncertainties on model outputs. This is in a similar spirit of Baroni and Tarantola (2014), who developed a general probabilistic framework to considering all uncertainty sources in global sensitivity analysis. Their framework however does not specify the hierarchical structure from model scenarios to model structures and to model parameters. Since various frameworks of uncertainty quantification have been developed for different purposes of hydrologic modeling (Matott et al., 2009; Renard et al., 2010; Refsgaard et al., 2012; Tartakovsky, 2013), our method of global sensitivity analysis may be extended to the different frameworks to meet the various needs of global sensitivity analysis.

Another focus of this paper is to use computationally efficient methods for global sensitivity analysis, which is well known to be computationally expensive because it requires Monte Carlo (MC) simulation with a large number of model executions (Sobol', 1993; Jansen, 1999; Sobol' et al., 2007; Saltelli et al., 2010). Various methods have been developed to reduce the computational cost. A common practice is to first conduct a Morris analysis to screen out unimportant parameters so that global sensitivity analysis is only conducted for important parameters (e.g., Chu-Agor et al. 2011; Zhao et al., 2011). The quasi-random sampling method developed by Saltelli et al. (2010) is the most popular MC method because the number of model executions needed for Sobol' sensitivity analysis is dramatically reduced in comparison with conventional MC methods. Rakovec et al. (2014) developed a hybrid local-global sensitivity analysis method termed the Distributed Evaluation of Local Sensitivity Analysis (DELSA) to implement Sobol' sensitivity analysis. DELSA is computationally efficient, because it does not use MC methods but uses the results of local sensitivity analysis (i.e., the Jacobian matrix) to approximate the Sobol' variance terms. Another kind of widely used methods is meta-modeling to build cheap-to-compute surrogates or emulators of computationally expensive models so that performing a large number of model executions is computationally affordable (O'Hagan, 2006). The methods of developing surrogates for sensitivity analysis include Taylor series approximation (Hakami et al., 2003), response surface approximation (Helton and Davis, 2003), Fourier series (Saltelli et al., 1999) nonparametric regression (Helton, 1993; Storlie et al., 2009), Kriging (Kleijnen, 2009; Borgonovo et al., 2012; Lamoureaux et al., 2014), Gauss process (Rasmussen and Williams, 2006), polynomial chaos expansion (Garcia-Cabrejo and Valocchi, 2014; Formaggia et al., 2013; Oladyshkin et al., 2012; Sudret, 2007), and sparse-grid collocation (Buzzard, 2012; Buzzard and Xiu, 2011). However, the meta-modeling methods may still need a relatively large number of model executions to develop accurate surrogates, and the surrogate development is not always straightforward due to model non-linearity (Razavi et al., 2012; Zhang et al., 2013a, 2013b). Therefore, there are still urgent needs to develop new computationally efficient methods for performing global sensitivity analysis.

This paper presents a use of the computationally efficient method based on sparse grid collocation (SGC) techniques for variance-based global sensitivity analysis. The SGC techniques were developed for computing multidimensional integration (Smolyak, 1963), and have been shown to be an efficient and effective tool to overcome the curse of dimensionality for high dimensional numerical integration and interpolation (Barthelmann et al., 1999; Bungartz and Griebel, 2004; Gerstner and Griebel, 1998; Xiu and Hesthaven, 2005). The SGC techniques are particularly suitable for variance-based global sensitivity analysis, because the mean and variance needed for the sensitivity analysis are multivariate integrals. Based on quadrature rules (e.g., Gerstner and Griebel, 1998), SGC evaluates mean and variance of a quantity of interest at selected sparse grid points in parameter space. Since the number of

sparse grid points is always small, the corresponding number of model executions is small. This use of SGC is similar to SGC applications to moment equations for estimating mean and variance using quadrature rules directly without building surrogates (Lin and Tartakovsky, 2009, 2010; Lin et al., 2010; Shi et al., 2009).

In the rest of this paper, we present in Section 2 the new method of variance-based global sensitivity analysis for multiple models and scenarios, followed by its SGC implementation. An example application of the new method is demonstrated using a synthetic case of groundwater flow and reactive transport modeling described in Section 3. The results discussed in Section 4 show that the new global sensitivity indices can be used to avoid biased selection of influential parameters. Section 4 also investigates dependence of the sensitivity analysis results on model and scenario probability in the numerical example. In addition, accuracy of the SGC method is evaluated by comparing the SGC results with those obtained using the quasi-random sampling method of Saltelli et al. (2010). Conclusions of this research are given in Section 5.

2. Methodology

This section starts with the conventional definition of the global sensitivity indices for a single model and a single scenario, followed by the new definitions for multiple models but a single scenario and for multiple models and multiple scenarios. Subsequently, the SGC algorithm of evaluating the indices is presented together with the quasi-random sampling method of Saltelli et al. (2010).

2.1. Conventional definition of global sensitivity indices

In the conventional variance-based global sensitivity analysis that considers a single model and a single scenario, global sensitivity indices are evaluated as a quantitative measure of parameter influence on model outputs (Saltelli et al., 1999; Saltelli et al., 1998; Sobol', 1993). For a model with the form of $\Delta = f(\theta) = f(\theta_1, \dots, \theta_d)$, where Δ is a scalar model output and $\theta = \{\theta_1, \dots, \theta_d\}$ denotes the vector of model parameters, the total output variance, V , of Δ can be decomposed as (Sobol', 1993)

$$V(\Delta) = \sum_{i=1}^d V_i + \sum_{i=1}^d \sum_{j>i}^d V_{i,j} + \dots + V_{1,\dots,d}, \quad (1)$$

where V_i represents the partial variances contributed by parameter θ_i , and $V_{i,j}$ to $V_{1,\dots,k}$ represent the partial variances caused by interactions among the parameters.

The first-order sensitivity index of parameter θ_i is defined as (Sobol', 1993)

$$S_i = \frac{V_i}{V(\Delta)}, \quad (2)$$

which measures the main or first-order effect of the parameter θ_i on the model output. The index can also be defined by using the law of total variance to express the total variance as

$$V(\Delta) = V_{\theta_i}(E_{\theta_{\sim i}}(\Delta|\theta_i)) + E_{\theta_i}(V_{\theta_{\sim i}}(\Delta|\theta_i)), \quad (3)$$

The first term at the right hand side is the partial variance or the main effect caused by θ_i , and the inner expectation is the mean of the output calculated using all the changing values of parameter vector, $\theta_{\sim i}$, i.e., all parameters except fixed θ_i . Eq. (3) leads to the first-order sensitivity index

$$S_i = \frac{V_{\theta_i}(E_{\theta_{\sim i}}(\Delta|\theta_i))}{V(\Delta)}. \quad (4)$$

Homma and Saltelli (1996) introduced another important and widely used global sensitivity index, the total sensitivity index, as

$$S_{T_i} = \frac{V_i + V_{i,j} + \dots + V_{i,j,\dots,k}}{V(\Delta)}. \quad (5)$$

It considers both the first-order effect of θ_i and the interactions of θ_i with other parameters. In order to calculate the total sensitivity index, the total variance is decomposed as

$$V(\Delta) = V_{\theta_{\sim i}}(E_{\theta_i}(\Delta|\theta_{\sim i})) + E_{\theta_{\sim i}}(V_{\theta_i}(\Delta|\theta_{\sim i})), \quad (6)$$

where the first term at the right hand side measures the variance induced by $\theta_{\sim i}$. With Eq. (6), S_{T_i} can be defined by ruling out the partial variance as

$$S_{T_i} = \frac{E_{\theta_{\sim i}}(V_{\theta_i}(\Delta|\theta_{\sim i}))}{V(\Delta)} = \frac{V(\Delta) - V_{\theta_{\sim i}}(E_{\theta_i}(\Delta|\theta_{\sim i}))}{V(\Delta)}. \quad (7)$$

2.2. Global sensitivity indices for multiple models and scenarios

When considering model and scenario uncertainty, the total variance of model output can be expressed as (Appendix A)

$$V(\Delta) = E_S E_{\mathbf{M}|\mathbf{S}} E_{\mathbf{0}|\mathbf{M},\mathbf{S}} V(\Delta|\mathbf{0}, \mathbf{M}, \mathbf{S}) + E_S E_{\mathbf{M}|\mathbf{S}} V_{\mathbf{0}|\mathbf{M},\mathbf{S}} E(\Delta|\mathbf{0}, \mathbf{M}, \mathbf{S}) + E_S V_{\mathbf{M}|\mathbf{S}} E_{\mathbf{0}|\mathbf{M},\mathbf{S}} E(\Delta|\mathbf{0}, \mathbf{M}, \mathbf{S}) + V_S E_{\mathbf{M}|\mathbf{S}} E_{\mathbf{0}|\mathbf{M},\mathbf{S}} E(\Delta|\mathbf{0}, \mathbf{M}, \mathbf{S}), \quad (8)$$

where \mathbf{M} and \mathbf{S} are the sets of individual models, M , and individual scenarios, S , respectively, and $\mathbf{M}|\mathbf{S}$ and $\mathbf{0}|\mathbf{M},\mathbf{S}$ indicate the hierarchical relations that models are conditioned on scenarios and that parameters are conditioned on models and scenarios. Eq. (8) does not require that different scenarios have the same models. Instead, \mathbf{M} is a union of all the models specific to the scenarios. For example, considering that models M_1 and M_2 are associated with scenario 1 (S_1) and models M_1 and M_3 with scenario 2 (S_2), \mathbf{M} is a union of all the models, i.e., $\mathbf{M} = \{M_1, M_2, M_3\}$. Similarly, different models can have different parameters, and $\theta = \theta^{(1)} \cup \theta^{(2)} \dots \cup \theta^{(k)}$, where $\theta^{(k)}$ is the parameters of model M_k . These notations are used below for evaluating the sensitivity indices. The total variance is decomposed into data variance, $E_S E_{\mathbf{M}|\mathbf{S}} E_{\mathbf{0}|\mathbf{M},\mathbf{S}} V(\Delta|\mathbf{0}, \mathbf{M}, \mathbf{S})$, parametric variance, $E_S E_{\mathbf{M}|\mathbf{S}} V_{\mathbf{0}|\mathbf{M},\mathbf{S}} E(\Delta|\mathbf{0}, \mathbf{M}, \mathbf{S})$, model variance, $E_S V_{\mathbf{M}|\mathbf{S}} E_{\mathbf{0}|\mathbf{M},\mathbf{S}} E(\Delta|\mathbf{0}, \mathbf{M}, \mathbf{S})$, and scenario variance, $V_S E_{\mathbf{M}|\mathbf{S}} E_{\mathbf{0}|\mathbf{M},\mathbf{S}} E(\Delta|\mathbf{0}, \mathbf{M}, \mathbf{S})$. The data variance here is treated as the variance of measurement error. Since it is independent of model parameters, structures, and scenarios (i.e., $E_S E_{\mathbf{M}|\mathbf{S}} E_{\mathbf{0}|\mathbf{M},\mathbf{S}} V(\Delta|\mathbf{0}, \mathbf{M}, \mathbf{S}) = V(\Delta|\mathbf{0}, \mathbf{M}, \mathbf{S}) = C$), the data variance is a constant and not involved in the sensitivity analysis. The $E(\Delta|\mathbf{0}, \mathbf{M}, \mathbf{S})$ term is the model output of Δ given by a model under its associated parameters and scenario. While the meaning of $E(\Delta|\mathbf{0}, \mathbf{M}, \mathbf{S})$ and $V(\Delta|\mathbf{0}, \mathbf{M}, \mathbf{S})$ may change for a stochastic model (e.g., kriging in Neuman et al., 2012; Lu et al., 2011, 2012), discussing it is beyond the scope of this study.

When observations, \mathbf{D} , of system parameters (e.g., hydraulic conductivity) and system state variables (e.g., hydraulic head) are available, they can be used in Eq. (8) to evaluate the conditional mean and variance by adding \mathbf{D} to every term of Eq. (8). For example, $V(\Delta)$ and $V(\Delta|\mathbf{0}, \mathbf{M}, \mathbf{S})$ become $V(\Delta|\mathbf{D})$ and $V(\Delta|\mathbf{D}, \mathbf{0}, \mathbf{M}, \mathbf{S})$, respectively. Using the conditioning data also change the way of calculating the means and variances at the right hand side of Eq. (8). The current means and variances in Eq. (8) are unconditional evaluated using the priors; after using \mathbf{D} to estimate the posterior weights (e.g., Schoniger et al., 2014) and conditional predictions (e.g., Lu et al., 2014), they become conditional statistics. Since evaluating the posteriors and conditional statistics are beyond the scope of this study, the priors are used in this study to demonstrate our methods.

In this paper, the global sensitivity analysis is focused only on $E_S E_{\mathbf{M}|\mathbf{S}} V_{\mathbf{0}|\mathbf{M},\mathbf{S}} E(\Delta|\mathbf{0}, \mathbf{M}, \mathbf{S})$, because the other three variance terms are not caused by parametric uncertainty. With the introduced hierarchical structure and notations of models and scenarios, the first-order sensitivity index and total sensitivity index are redefined below.

2.2.1. Global sensitivity indices for single model and single scenario

When considering a single model, M , and a single scenario, S , $E_S E_{M|S} V_{\theta_i|M,S} E(\Delta|\theta, \mathbf{M}, \mathbf{S})$ becomes $V_{\theta_i|M,S} E(\Delta|\theta, M, S)$. Similar to Eq. (3), the variance due to parametric uncertainty is decomposed as

$$V_{\theta_i|M,S} E(\Delta|\theta, M, S) = V_{\theta_i|M,S} E_{\theta_{-i}|M,S} (E(\Delta|\theta, M, S)|\theta_i) + E_{\theta_{-i}|M,S} V_{\theta_{-i}|M,S} (E(\Delta|\theta, M, S)|\theta_i), \tag{9}$$

and the first-order sensitivity index is defined as

$$S_i = \frac{V_{\theta_i|M,S} E_{\theta_{-i}|M,S} (E(\Delta|\theta, M, S)|\theta_i)}{V_{\theta_i|M,S} E(\Delta|\theta, M, S)}. \tag{10}$$

Similarly, Eq. (6) can be rewritten as

$$V_{\theta_i|M,S} E(\Delta|\theta, M, S) = E_{\theta_{-i}|M,S} V_{\theta_i|M,S} (E(\Delta|\theta, M, S)|\theta_{-i}) + V_{\theta_{-i}|M,S} E_{\theta_i|M,S} (E(\Delta|\theta, M, S)|\theta_{-i}), \tag{11}$$

and the total sensitivity index is defined as

$$S_{T_i} = \frac{E_{\theta_{-i}|M,S} V_{\theta_i|M,S} (E(\Delta|\theta, M, S)|\theta_{-i})}{V_{\theta_i|M,S} E(\Delta|\theta, M, S)} = 1 - \frac{V_{\theta_{-i}|M,S} E_{\theta_i|M,S} (E(\Delta|\theta, M, S)|\theta_{-i})}{V_{\theta_i|M,S} E(\Delta|\theta, M, S)}. \tag{12}$$

2.2.2. Global sensitivity indices for multiple models and single scenario

When considering multiple models, \mathbf{M} , but a single scenario, S , $E_S E_{M|S} V_{\theta_i|M,S} E(\Delta|\theta, \mathbf{M}, \mathbf{S})$ becomes $E_{M|S} V_{\theta_i|M,S} E(\Delta|\theta, \mathbf{M}, \mathbf{S})$. It can be decomposed as

$$E_{M|S} V_{\theta_i|M,S} E(\Delta|\theta, \mathbf{M}, \mathbf{S}) = E_{M|S} E_{\theta_{-i}|M,S} V_{\theta_i|M,S} (E(\Delta|\theta, \mathbf{M}, \mathbf{S})|\theta_i) + E_{M|S} V_{\theta_{-i}|M,S} E_{\theta_i|M,S} (E(\Delta|\theta, \mathbf{M}, \mathbf{S})|\theta_i) \tag{13}$$

or

$$E_{M|S} V_{\theta_i|M,S} E(\Delta|\theta, \mathbf{M}, \mathbf{S}) = E_{M|S} E_{\theta_{-i}|M,S} V_{\theta_i|M,S} (E(\Delta|\theta, \mathbf{M}, \mathbf{S})|\theta_{-i}) + E_{M|S} V_{\theta_{-i}|M,S} E_{\theta_i|M,S} (E(\Delta|\theta, \mathbf{M}, \mathbf{S})|\theta_{-i}) \tag{14}$$

Accordingly, the first-order and total sensitivity indices for multiple models are defined as

$$S_i^M = \frac{E_{M|S} V_{\theta_i|M,S} E_{\theta_{-i}|M,S} (E(\Delta|\theta, \mathbf{M}, \mathbf{S})|\theta_i)}{E_{M|S} V_{\theta_i|M,S} E(\Delta|\theta, \mathbf{M}, \mathbf{S})} \tag{15}$$

and

$$S_{T_i}^M = \frac{E_{M|S} E_{\theta_{-i}|M,S} V_{\theta_i|M,S} (E(\Delta|\theta, \mathbf{M}, \mathbf{S})|\theta_{-i})}{E_{M|S} V_{\theta_i|M,S} E(\Delta|\theta, \mathbf{M}, \mathbf{S})} \tag{16}$$

Eqs. (15) and (16) take into account the parameter influence under the individual models, and provide a quantitative assessment of global sensitivity analysis with combined effects of uncertain parameters and models. Comparing Eqs. (15) and (16) with Eqs. (11) and (12), respectively, shows that S_T^M of multiple models is not a weighted average of S_T of individual models, because model averaging is conducted for the variance of individual models not for the index of individual models.

The mean of multiple models, $E_{M|S}(\cdot)$, in Eqs. (15) and (16), is evaluated by the weighted average, i.e., $E_{M|S}(\cdot) = \sum_k P(M_k|S)(\cdot)$, where $P(M_k|S)$ is the probability of model M_k under scenario S and satisfies $\sum_k P(M_k|S) = 1$. Based on the model averaging concept, Eq. (15) is evaluated as

$$S_i^M = \frac{\sum_k P(M_k|S) V_{\theta_i|M_k,S} E_{\theta_{-i}|M_k,S} (E(\Delta|\theta, M_k, S)|\theta_i)}{\sum_k P(M_k|S) V_{\theta_i|M_k,S} E(\Delta|\theta, M_k, S)} \tag{17}$$

If parameter θ_i does not belong to model M_k , the $V_{\theta_i|M_k,S} E_{\theta_{-i}|M_k,S} (E(\Delta|\theta, M_k, S)|\theta_i)$ term is zero and $S_i^{M_k} = 0$, because uncertainty in θ_i does not contribute to the predictive uncertainty of model M_k . Similarly, the total sensitivity index is evaluated as

$$S_{T_i}^M = \frac{\sum_k P(M_k|S) E_{\theta_{-i}|M_k,S} V_{\theta_i|M_k,S} (E(\Delta|\theta, M_k, S)|\theta_{-i})}{\sum_k P(M_k|S) V_{\theta_i|M_k,S} E(\Delta|\theta, M_k, S)} \tag{18}$$

Similarly, If parameter θ_i does not belong to model M_k , the $V_{\theta_i|M_k,S} (E(\Delta|\theta, M_k, S)|\theta_{-i})$ term is zero and $S_{T_i}^{M_k} = 0$.

2.2.3. Global sensitivity indices for multiple models and multiple scenarios

When considering multiple models, \mathbf{M} , and multiple scenarios, \mathbf{S} , $E_S E_{M|S} V_{\theta_i|M,S} E(\Delta|\theta, \mathbf{M}, \mathbf{S})$ is decomposed as

$$E_S E_{M|S} V_{\theta_i|M,S} E(\Delta|\theta, \mathbf{M}, \mathbf{S}) = E_S E_{M|S} E_{\theta_{-i}|M,S} V_{\theta_i|M,S} (E(\Delta|\theta, \mathbf{M}, \mathbf{S})|\theta_i) + E_S E_{M|S} V_{\theta_i|M,S} E_{\theta_{-i}|M,S} (E(\Delta|\theta, \mathbf{M}, \mathbf{S})|\theta_i) \tag{19}$$

and

$$E_S E_{M|S} V_{\theta_i|M,S} E(\Delta|\theta, \mathbf{M}, \mathbf{S}) = E_S E_{M|S} E_{\theta_{-i}|M,S} V_{\theta_i|M,S} (E(\Delta|\theta, \mathbf{M}, \mathbf{S})|\theta_{-i}) + E_S E_{M|S} V_{\theta_{-i}|M,S} E_{\theta_i|M,S} (E(\Delta|\theta, \mathbf{M}, \mathbf{S})|\theta_{-i}) \tag{20}$$

Accordingly, the first-order and total sensitivity indices for multiple models and multiple scenarios are defined as

$$S_i^{MS} = \frac{E_S E_{M|S} V_{\theta_i|M,S} E_{\theta_{-i}|M,S} (E(\Delta|\theta, \mathbf{M}, \mathbf{S})|\theta_i)}{E_S E_{M|S} V_{\theta_i|M,S} E(\Delta|\theta, \mathbf{M}, \mathbf{S})} = \frac{\sum_S \sum_M P(S) P(M|S) V_{\theta_i|M,S} E_{\theta_{-i}|M,S} (E(\Delta|\theta, \mathbf{M}, \mathbf{S})|\theta_i)}{\sum_S \sum_M P(S) P(M|S) V_{\theta_i|M,S} E(\Delta|\theta, \mathbf{M}, \mathbf{S})} \tag{21}$$

and

$$S_{T_i}^{MS} = \frac{E_S E_{M|S} E_{\theta_{-i}|M,S} V_{\theta_i|M,S} (E(\Delta|\theta, \mathbf{M}, \mathbf{S})|\theta_{-i})}{E_S E_{M|S} V_{\theta_i|M,S} E(\Delta|\theta, \mathbf{M}, \mathbf{S})} = \frac{\sum_S \sum_M P(S) P(M|S) E_{\theta_{-i}|M,S} V_{\theta_i|M,S} (E(\Delta|\theta, \mathbf{M}, \mathbf{S})|\theta_{-i})}{\sum_S \sum_M P(S) P(M|S) V_{\theta_i|M,S} E(\Delta|\theta, \mathbf{M}, \mathbf{S})} \tag{22}$$

Eqs. (21) and (22) take into account the parameter influence under the individual models and individual scenarios, and provide a quantitative assessment of global sensitivity analysis with combined effects of uncertain parameters, models, and scenarios. Again, S_T^{MS} of multiple scenarios is not a weighted average of S_T^M of individual scenarios.

Similar to the concept of model averaging, scenario averaging is applied here by evaluating the mean for multiple scenarios, $E_S(\cdot)$, by the weighted average, i.e., $E_S(\cdot) = \sum_i P(S_i)(\cdot)$, where $P(S)$ is scenario probability and satisfies $\sum_i P(S_i) = 1$. Using the concepts of model averaging and scenario averaging, Eq. (21) can be evaluated as

$$S_i^{MS} = \frac{\sum_i \sum_k P(S_i) P(M_k|S_i) V_{\theta_i|M_k,S_i} E_{\theta_{-i}|M_k,S_i} (E(\Delta|\theta, M_k, S_i)|\theta_i)}{\sum_i \sum_k P(S_i) P(M_k|S_i) V_{\theta_i|M_k,S_i} E(\Delta|\theta, M_k, S_i)} \tag{23}$$

If parameter θ_i does not belong to model M_k and scenario S_i , $V_{\theta_i|M_k,S_i} E_{\theta_{-i}|M_k,S_i} (E(\Delta|\theta, M_k, S_i)|\theta_i)$ is zero, and $S_i^{M_k S_i} = 0$. Similarly, the total sensitivity index is evaluated as

$$S_{T_i}^{MS} = \frac{\sum_i \sum_k P(S_i) P(M_k|S_i) E_{\theta_{-i}|M_k,S_i} V_{\theta_i|M_k,S_i} (E(\Delta|\theta, M_k, S_i)|\theta_{-i})}{\sum_i \sum_k P(S_i) P(M_k|S_i) V_{\theta_i|M_k,S_i} E(\Delta|\theta, M_k, S_i)} \tag{24}$$

If parameter θ_i does not belong to model M_k and scenario S_i , $V_{\theta_i|M_k,S_i} (E(\Delta|\theta, M_k, S_i)|\theta_{-i})$ is zero, and $S_{T_i}^{M_k S_i} = 0$.

2.3. SGC-based evaluation of global sensitivity indices

Evaluation of the global sensitivity indices requires calculating the mean and variance with respect to model parameters as well as the probabilities of models and scenarios. Since various methods of estimating model and scenario probabilities have been developed, they are not discussed in this paper. This paper is focused on evaluating the mean and variance with respect to model parameters using the SGC methods. Since the SGC methods are applied in

the parameter space of each model under each scenario, for the convenience of mathematical expression, we drop all the notations of conditioning on models and scenarios, and use again the notations of $V_{\theta_i}(E_{\theta_{-i}}(\Delta|\theta_i))$ and $E_{\theta_{-i}}(V_{\theta_i}(\Delta|\theta_{-i}))$.

The quasi-random sampling method is the most computationally efficient MC methods so far for evaluating the first-order and total sensitivity indices. Following Jansen (1999) and Saltelli et al. (2010), the mean and variance are evaluated via

$$V_{\theta_i}(E_{\theta_{-i}}(\Delta|\theta_i)) = \frac{1}{n} \sum_{j=1}^n f(\mathbf{B}_j)(f(\mathbf{A}_{\mathbf{B},j}^i) - f(\mathbf{A}_j)), \tag{25}$$

and

$$E_{\theta_{-i}}(V_{\theta_i}(\Delta|\theta_{-i})) = \frac{1}{2n} \sum_{j=1}^n (f(\mathbf{A}_j) - f(\mathbf{A}_{\mathbf{B},j}^i))^2, \tag{26}$$

where $\Delta = f(\cdot)$ denote a model execution for its parameters. The calculation requires two independent parameter sample matrices, \mathbf{A} and \mathbf{B} , with the same dimension of $n \times d$, where n is number of samples and d is number of parameters. Matrix $\mathbf{A}_{\mathbf{B}}^i$ is the same as matrix \mathbf{A} except that its i th column is from the i th column of matrix \mathbf{B} . Subscript j denotes the j th row of the corresponding matrix, i.e., the j th sample of the parameters. A MC implementation of Eqs. (21) and (22) requires $(2 + d)n$ times of model executions, i.e., $2n$ executions corresponding to matrices \mathbf{A} and \mathbf{B} and dn executions using matrix $\mathbf{A}_{\mathbf{B}}^i$. While the total number of model executions only increases linearly with the number of model parameters, it is still computationally expensive, because the number of samples must be sufficiently large to attain convergence of the MC simulation.

Our computationally efficient SGC algorithm is rooted in the quadrature rules of numerical integration. Starting from an integral of a one-dimensional function $g(x)$, the general quadrature formula is (Gerstner and Griebel, 1998):

$$Qg := \sum_{i=1}^N \omega_i g(x_i) \tag{27}$$

where x_i are parameter values (i.e., quadrature points) chosen following a quadrature rule, ω_i are corresponding weights, and N is number of quadrature points. For a d -dimensional function f , the tensor product of d quadrature formulas ($Q_{l_1} \otimes \dots \otimes Q_{l_d}$) is

$$(Q_{l_1} \otimes \dots \otimes Q_{l_d})f := \sum_{i_1=1}^{N_{l_1}} \dots \sum_{i_d=1}^{N_{l_d}} \omega_{i_1 i_1} \dots \omega_{i_d i_d} f(x_{i_1 i_1}, \dots, x_{i_d i_d}) \tag{28}$$

where $x_{i_1 i_1}, \dots, x_{i_d i_d}$ are quadrature points chosen by a quadrature rule, l_1, \dots, l_d are the precision levels for the quadrature rule, $\omega_{i_1 i_1}, \dots, \omega_{i_d i_d}$ are corresponding weights, N_{l_1}, \dots, N_{l_d} are number of quadrature points for each dimension. The tensor product is still computationally expensive, because it suffers from the curse of dimensionality, i.e., the number of model executions increases exponentially with the number of model parameters. This problem can be resolved by using the sparse grid collocation method. Define a multi-index $k = (k_1, \dots, k_d) \in \mathbb{N}^d$ with the norm of $\|k\| = k_1 + \dots + k_d$. Instead of using the full tensor product quadrature rule, following the Smolyak or sparse grid cubature rule, a d -dimensional function integral with precision level l can be approximated by (Gerstner and Griebel, 1998):

$$I(l, d)[f] = \sum_{l+1 \leq \|k\| \leq l+d} (-1)^{l+d-\|k\|} \binom{d-1}{\|k\|-l-1} (Q_{k_1} \otimes \dots \otimes Q_{k_d})f \tag{29}$$

The number of model executions reduces from N^d for the full tensor product to $\frac{(2d)^l}{l!}$ for the sparse grid tensor product (Novak and Ritter, 1999). The determination of precision level l has been discussed in Gerstner and Griebel (1998, 2003).

The SGC algorithm is flexible for global sensitivity analysis, because it allows using different quadrature rules for different shapes of parameter distributions. In this paper, the Clenshaw–Curtis rule is chosen for uniform parameter distribution. The quadrature points and weights of this rule for the integral $\int_{-1}^1 g(x)dx$ are (Davis and Rabinowitz, 1975):

$$x_i = \cos\left(\frac{i\pi}{N}\right), \quad i = 0, 1, \dots, N$$

$$\omega_0 = \omega_N = \frac{1}{N^2-1}$$

$$\omega_s = \omega_{N-s} = \frac{2}{N} \left(1 + \frac{1}{1-N^2} \cos \pi s + \sum_{j=1}^{N/2-1} \frac{2}{1-4j^2} \cos \frac{2j\pi s}{N} \right), \quad s = 1, \dots, \frac{N}{2}. \tag{30}$$

where N is an even number. The Gauss–Hermite rule is chosen for the normal parameter distribution. For the integral $\int_{-\infty}^{\infty} e^{-x^2} g(x)dx$, the quadrature points are the solution of Hermite polynomial, $H_N(x)$, and weights are (Davis and Rabinowitz, 1967):

$$\omega_i = \frac{2^{N+1} N! \sqrt{\pi}}{[H_{N+1}(x_i)]^2} \tag{31}$$

In practical applications, if the integrals are different from the standard forms above for which the SGC quadrature rules were developed, change of variable is required to transform the integrals into the standard forms. Take as an example of evaluating the mean of function $h(y)$ with respect to random variable y that follows the normal distribution $N(\mu, \sigma)$,

$$E[h(y)] = \int_{-\infty}^{\infty} \frac{1}{\sigma\sqrt{2\pi}} \exp\left(-\frac{(y-\mu)^2}{2\sigma^2}\right) h(y) dy. \tag{32}$$

In order to use the Gauss–Hermite rule developed for the standard form of $\int_{-\infty}^{\infty} e^{-x^2} g(x)dx$, a change of variable is needed by defining

$$x = \frac{y-\mu}{\sqrt{2}\sigma} \quad \text{and} \quad y = \sqrt{2}\sigma x + \mu, \tag{33}$$

with which Eq. (32) becomes

$$E[h(y)] = \int_{-\infty}^{\infty} \frac{1}{\sigma\sqrt{2\pi}} \exp(-x^2) h(\sqrt{2}\sigma x + \mu) dy$$

$$= \frac{1}{\sqrt{\pi}} \int_{-\infty}^{\infty} \exp(-x^2) h(\sqrt{2}\sigma x + \mu) dx. \tag{34}$$

Applying the Gauss–Hermite rule to Eq. (34) leads to

$$E[h(y)] = \frac{1}{\sqrt{\pi}} \sum_{i=1}^n \omega_i h(\sqrt{2}\sigma x_i + \mu). \tag{35}$$

The quadrature points and corresponding weights of other parameter distributions can be found in Davis and Rabinowitz (1967, 1975).

To evaluate $V_{\theta_i}(E_{\theta_{-i}}(\Delta|\theta_i))$ defined in Eq. (4),

$$V_{\theta_i}(E_{\theta_{-i}}(\Delta|\theta_i)) = E_{\theta_i} \left((E_{\theta_{-i}}(\Delta|\theta_i))^2 \right) - (E_{\theta_i}(E_{\theta_{-i}}(\Delta|\theta_i)))^2, \tag{36}$$

for the first-order sensitivity index, three sparse grid integrations are needed. The first one approximates $E_{\theta_{-i}}(\Delta|\theta_i)$ as

$$E_{\theta_{-i}}(\Delta|\theta_i) \approx \mathbf{I}_1(l_1, d-1)[f(\boldsymbol{\theta}_{-i})], \tag{37}$$

where l_1 is the level of precision of \mathbf{I}_1 . Note that the dimension is $d-1$ for $\boldsymbol{\theta}_{-i}$, because θ_i is fixed. The second sparse grid approximates $E_{\theta_i}((E_{\theta_{-i}}(\Delta|\theta_i))^2)$ as

$$E_{\theta_i}((E_{\theta_{-i}}(\Delta|\theta_i))^2) \approx \mathbf{I}_2(l_2, 1)[(\mathbf{I}_1(l_1, d-1)[f(\boldsymbol{\theta}_{-i})])^2], \tag{38}$$

where l_2 is the level of precision of \mathbf{I}_2 . Since the integral has only one random variable, θ_i , the dimension of \mathbf{I}_2 is 1. $E_{\theta_i}(E_{\theta_{-i}}(\Delta|\theta_i))$ is approximated as

$$E_{\theta_i}(E_{\theta_{-i}}(\Delta|\theta_i)) \approx \mathbf{I}_3(l_3, 1)[\mathbf{I}_1(l_1, d - 1)[f(\theta_{-i})]] \quad (39)$$

where \mathbf{I}_3 is another sparse grid with precision level l_3 .

To evaluate $E_{\theta_{-i}}(V_{\theta_i}(\Delta|\theta_{-i}))$ for the total sensitivity index defined in Eq. (7), sparse grid \mathbf{I}_4 is developed as:

$$E_{\theta_{-i}}(V_{\theta_i}(\Delta|\theta_{-i})) \approx \mathbf{I}_4(l_4, d - 1)[V_{\theta_i}(\Delta|\theta_{-i})] \quad (40)$$

where l_4 is the level of precision of \mathbf{I}_4 . By developing another two sparse grids for $V_{\theta_i}(\Delta|\theta_{-i}) = E_{\theta_i}(\Delta^2|\theta_{-i}) - (E_{\theta_i}(\Delta|\theta_{-i}))^2$, Eq. (40) becomes

$$E_{\theta_{-i}}(V_{\theta_i}(\Delta|\theta_{-i})) \approx \mathbf{I}_4(l_4, d - 1)[\mathbf{I}_5(l_5, 1)[f^2(\theta_i)] - (\mathbf{I}_6(l_6, 1)[f(\theta_i)])^2] \quad (41)$$

where \mathbf{I}_5 and \mathbf{I}_6 are two new sparse grids with precision levels of l_5 and l_6 , respectively. To save computational cost, the total variance of output Δ is not evaluated by building new sparse grids but by using existing sparse grids as follows

$$\begin{aligned} V(\Delta) &= E(\Delta^2) - (E(\Delta))^2 = E_{\theta_{-i}}(E_{\theta_i}(\Delta^2|\theta_{-i})) - (E_{\theta_i}(E_{\theta_{-i}}(\Delta|\theta_i)))^2 \\ &\approx \mathbf{I}_4(l_4, d - 1)[\mathbf{I}_5(l_5, 1)[f^2(\theta_i)] - (\mathbf{I}_3(l_3, 1)[\mathbf{I}_1(l_1, d - 1)[f(\theta_{-i})]])^2 \end{aligned} \quad (42)$$

Therefore, the total number of model executions needed for calculating global sensitivity indices of a single parameter is $m_1m_2 + m_1 - m_3 + m_4m_5 + m_4m_6$, where m_1 and m_4 are the numbers of sparse grid points chosen for θ_{-i} , corresponding to levels l_1 and l_4 , respectively, and m_2, m_3, m_5 and m_6 are the numbers of sparse grid points chosen for θ_i , corresponding to levels l_2, l_3, l_5 and l_6 , respectively. Since the values of $m_1 - m_6$ are in general small, the total number of model executions is still significantly smaller than $(2 + d)n$ used in the quasi-random sampling method of MC simulations. The SGC algorithm is general in that it allows developing different sparse grids for different mean and variance terms involved in the variance-based global sensitivity analysis. However, the algorithm can be simplified by using the same sparse grid for different variance terms. In the numerical example demonstrated below in Section 3, instead of using six different sparse grids, only two sparse grids are used to calculate the sensitivity indices by using the same precision level for the sparse grid integration with the same parameters: one sparse grid for integration with θ_i and the other sparse grid for integration with θ_{-i} .

3. Synthetic case with multiple scenarios and models

The global sensitivity indices are evaluated for a synthetic case of groundwater reactive transport modeling with three scenarios, four models, and six random parameters. Only built for the purposes of demonstration and test, the synthetic case is relatively simple, which makes it computationally affordable to have millions of model executions for evaluating the indices using the MC method of Saltelli et al. (2010). The MC results are used as the reference to evaluate the accuracy of the SGC algorithm.

3.1. Synthetic case of groundwater reactive transport modeling

In the synthetic domain of groundwater flow shown in Fig. 1, the unconfined groundwater aquifer of length L is under a steady-state condition and has a uniform precipitation, P , over the entire domain. Specification of the precipitation and the groundwater flow models are given below. A continuous contaminant source is placed at the center of the domain ($x = 5000$ m). Similar to Chen et al. (2013), a total of five chemical species are involved in the reactive transport modeling, and they are PCE (perchloroethene), TCE (trichloroethene), DCE (dichloroethene), VC (vinyl chloride), and ETH (ethene). The single chain reactions

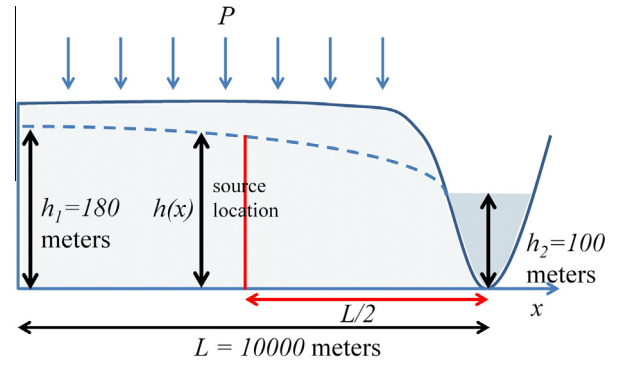


Fig. 1. Diagram of the modeling domain of the synthetic study. $L = 1000$ m is the domain length. Precipitation is uniform for the entire domain. Constant head (h) boundary conditions are $h_1 = 180$ m and $h_2 = 100$ m. The continuous contaminant source is located in the middle of the domain.



Fig. 2. Single chain reactions from PCE (perchloroethene), to TCE (trichloroethene), and DCE (cis-1,2-dichloroethylene), VC (Vinyl chloride), and ETH (Ethene).

(Fig. 2) described in the user's manual of BIOCHLOR (Aziz et al., 2000) are used in this study. The governing equations of the reactive transport modeling are:

$$\begin{aligned} \frac{\partial c_1}{\partial t} &= D \frac{\partial^2 c_1}{\partial x^2} - v \frac{\partial c_1}{\partial x} - k_1 c_1 \\ \frac{\partial c_2}{\partial t} &= D \frac{\partial^2 c_2}{\partial x^2} - v \frac{\partial c_2}{\partial x} + y_1 k_1 c_1 - k_2 c_2 \\ \frac{\partial c_3}{\partial t} &= D \frac{\partial^2 c_3}{\partial x^2} - v \frac{\partial c_3}{\partial x} + y_2 k_2 c_2 - k_3 c_3 \\ \frac{\partial c_4}{\partial t} &= D \frac{\partial^2 c_4}{\partial x^2} - v \frac{\partial c_4}{\partial x} + y_3 k_3 c_3 - k_4 c_4 \\ \frac{\partial c_5}{\partial t} &= D \frac{\partial^2 c_5}{\partial x^2} - v \frac{\partial c_5}{\partial x} + y_4 k_4 c_4 - k_5 c_5 \end{aligned} \quad (43)$$

where $c_1 - c_5$ [M/L³] are concentrations of PCE, TCE, DCE, VC, and ETH, respectively, D [L²/T] is hydrodynamic dispersion coefficient in the x direction, v [L/T] is seepage velocity, $k_1 - k_5$ [1/L] are first-order degradation coefficients of the five species, and $y_1 - y_4$ are yield coefficients of PCE, TCE, DCE, and VC, respectively. Since the velocity varies in space but constant velocity is needed to derive analytical solutions of Eq. (43), the averaged velocity is estimated as $v = \frac{\bar{q}}{\phi}$, where ϕ [-] is porosity, and \bar{q} [L/T] is harmonic mean of the specific discharge in the right half part of the domain (the half domain with pollution). The analytical solutions and their numerical implementation developed by Sun et al. (1999) are used in this study.

3.2. Uncertain scenarios, models, and parameters

The synthetic case considers three alternative scenarios of future precipitation. The three scenarios are wet, baseline, and dry scenarios, and they are referred to as Scenario 1, Scenario 2, and Scenario 3, respectively, for the convenience of discussion below. Precipitation of the baseline scenario (Scenario 2) is assumed to follow a normal distribution with the mean of 1,524 mm/year and standard deviation of 254 mm/year. In the wet and dry scenarios (Scenarios 1 and 3, respectively), the amount of precipitation is assigned to be 180% and 80% of the precipitation

of the baseline scenario, respectively. The three distributions are truncated at zero to ensure positive precipitation. The probability density functions (PDFs) of precipitation in the three scenarios are shown in Fig. 3. The figure shows that both the mean and the variance increase from the dry to the wet scenario.

Two alternative groundwater flow models were built for the synthetic domain. The first model (denoted as one-zone model or Z_1) is based on the assumption that the domain is homogeneous with a constant hydraulic conductivity value. The corresponding mathematical model is

$$\frac{d^2(h(x)^2)}{dx^2} = -\frac{2w}{K} \tag{44}$$

$$h(x=0) = h_1$$

$$h(x=L) = h_2$$

where h [L] is hydraulic head, x [L] is distance from the left end of the domain, K [L/T] is hydraulic conductivity constant over the domain, w [L/T] is groundwater recharge rate, and h_1 [L] and h_2 [L] are hydraulic head at the left and right sides of the domain, respectively. The analytical solution of Eq. (44) is (Fetter, 2001):

$$h(x) = \sqrt{h_1^2 - \frac{(h_1^2 - h_2^2)x}{L} + \frac{w}{K}(L-x)x} \tag{45}$$

Using Darcy's law, the analytical solution of specific discharge, q [L/T], is

$$q(x) = \frac{1}{h} \left(\frac{K(h_1^2 - h_2^2)}{2L} - w \left(\frac{L}{2} - x \right) \right). \tag{46}$$

The second groundwater flow model (denoted as two-zone model or Z_2) was built with the assumption that the modeling domain consists of two zones with the divide at the location of $x = 7000$ m. The corresponding mathematical model is

$$\frac{d}{dx} \left(Kh(x) \frac{dh(x)}{dx} \right) = -w \tag{47}$$

$$h(x=0) = h_1$$

$$h(x=L) = h_2$$

where $K = K_1$ [L/T] for $x \in [0, 7,000]$ and $K = K_2$ [L/T] for $x \in [7,000, L]$ are hydraulic conductivity of the two zones. This model was solved numerically using the finite difference method.

Two alternative groundwater recharge models were considered in this study to convert precipitation to groundwater recharge. Considering recharge model uncertainty is necessary in groundwater modeling, because various techniques of recharge estimation have been developed and their recharge estimates can be

substantially different (Scanlon et al., 2002). The first recharge model, denoted as R_1 , is

$$M_1 : w = \begin{cases} 16.88(P - 355.6)^{0.50} & P \geq 355.6 \\ 0 & \text{Otherwise} \end{cases} \tag{48}$$

This model is based on the mass-balance study of Thomas et al. (2009), which showed an exponential relation between precipitation and recharge. The other recharge model, denoted as R_2 , is adapted from Krishna (1987),

$$M_2 : w = \begin{cases} 0.15(P - 399.80) & P \geq 399.80 \\ 0 & \text{Otherwise} \end{cases} \tag{49}$$

which relies on a linear relationship between precipitation and recharge. The coefficients of the two models are chosen to give sufficiently different recharge estimates by the two models. Fig. 4 plots the PDFs of the recharge estimates of the two models (R_1 and R_2 denote models 1 and 2, respectively) under the three precipitation scenarios. The figure shows that the recharge estimate of recharge model R_1 is larger than that of recharge model R_2 . For recharge model R_2 with linear relation between precipitation and recharge, the uncertainty in the recharge estimate is proportional to uncertainty in precipitation.

Six parameters of the groundwater flow and transport models are considered to be random (model input factors are also treated as parameters in this study without loss of generality). The first parameter is the precipitation, and its distributions under the three scenarios are discussed earlier. The next three parameters are hydraulic conductivity, K , K_1 and K_2 (m/d), which are assumed to follow the normal distributions $N(15,1)$, $N(20,1)$ and $N(10,1)$, respectively. These three normal distributions are truncated at the lower bound of zero. Although using lognormal distributions for hydraulic conductivity is more realistic, using the normal distributions here is simply for method demonstration. Despite that the results of sensitivity analysis may change significantly, we do not expect that the change would invalidate our new sensitivity indices. The fifth random parameter is hydrodynamic dispersion coefficient (m²/d), and the uniform distribution $U(10,10.1)$ is assumed. The last parameter is first-order degradation coefficient for PCE (1/d), and the normal distribution $N(0.05,0.01)$ truncated at the lower bound of zero is assumed.

Combining the two recharge models and the two groundwater models gives a total of four alternative models listed in Table 1: R_1Z_1 , R_2Z_1 , R_2Z_2 , and R_2Z_2 ; each model has the same transport component given in Eq. (43). The manner of formulating the four models is similar to that of Ye et al. (2010a) for quantifying model uncertainty in conceptualizing recharge component and hydrostratigraphic framework of the Death Valley Regional Flow system. For the four models, parametric uncertainty is conditioned on

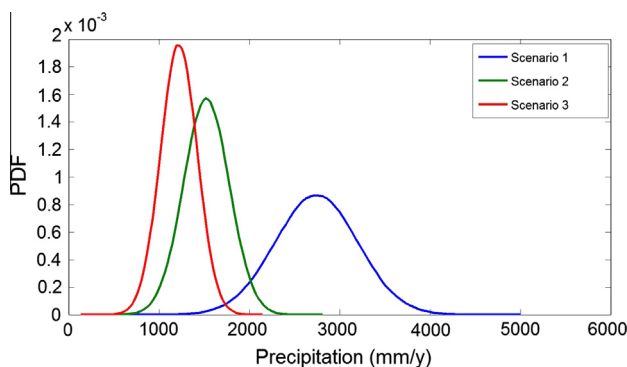


Fig. 3. Probability density functions (PDFs) of precipitation under three scenarios: Scenario 1 (wet), Scenario 2 (baseline), and Scenario 3 (dry).

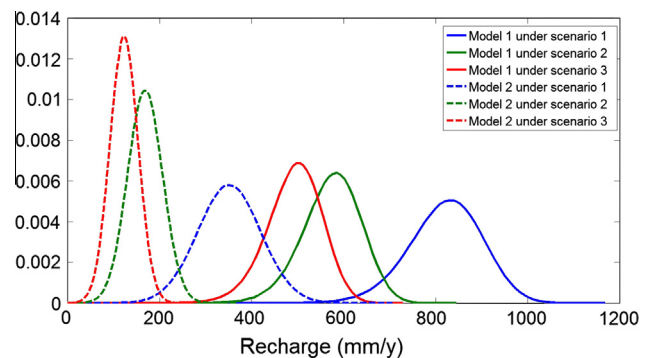


Fig. 4. Probability density functions (PDFs) of groundwater recharge given by two models (R_1 and R_2 denote models 1 and 2, respectively) under three precipitation scenarios.

model uncertainty, from the hierarchical viewpoint discussed before. For example, uncertainty of hydraulic conductivity K is for models R_1Z_1 and R_2Z_1 , and uncertainty of K_1 and K_2 are conditioned on models R_1Z_2 and R_2Z_2 . Our new sensitivity indices are defined general, and different models can have different parameters.

4. Results and discussions

Sections 4.1–4.4 discuss the total sensitivity index evaluated for hydraulic head and ethene concentration for individual models and individual scenarios, for multiple models (after model averaging) but individual scenarios, and for multiple models and multiple scenarios (after scenario averaging). Although both first-order and total sensitivity indices are used in global sensitivity analysis, only the total sensitivity index is discussed for the reason explained in Sections 4.1 and 4.4. The results of Sections 4.1–4.4 are based on equal model and scenario probabilities. Impacts of model and scenario probabilities on the global sensitivity indices are investigated in Section 4.5 by evaluating the indices for different sets of the model and scenario probabilities. All the results in Sections 4.1–4.5 are based on the quasi-random sampling method of Saltelli et al. (2010). Accuracy and computational efficiency of the sparse grid collocation method is discussed in Section 4.6 by comparing the results of the SGC method with those obtained from millions of MC simulations.

4.1. Total sensitivity index for head under individual models and scenarios

Table 1 lists the values of total sensitivity index (S_T) of precipitation (S_{T_p}) and hydraulic conductivity (S_{T_K} , $S_{T_{K_1}}$, and $S_{T_{K_2}}$) calculated for hydraulic head at the location of $x = 6,000$ m for the four models under the three scenarios. Because parameter K does not belong to models R_1Z_2 and R_2Z_2 and parameters K_1 and K_2 do not belong to models R_1Z_1 and R_2Z_1 , the corresponding index values are zero, as discussed in Section 2. The table shows that, for each model and scenario, the sum of the total sensitivity indices for all parameters is slightly larger than 1, indicating that the interaction between the two parameters has a negligible contribution to head uncertainty. As a result, the first-order sensitivity index is almost identical to the total sensitivity index. Therefore, only the results of total sensitivity index are presented and discussed.

Table 1 shows that the index values may vary substantially for different models and scenarios. For example, S_{T_p} ranges from 5.96% for Model R_2Z_2 under Scenario 3 to 92.98% for Mode R_2Z_1 under Scenario 3, indicating that the importance of precipitation changes dramatically from unimportant to the most important. If identification of important parameters is based on a single model and a single scenario (without considering model and scenario uncertainty), biased identification may occur. The variation of the total sensitivity index between different models and scenarios is physically meaningful. For the homogeneous models (R_1Z_1 and R_2Z_1), the increase of the index (S_{T_p}) of precipitation from Scenario 1 (wet scenario) to Scenario 3 (dry scenario) is attributed to the decrease of precipitation and thus groundwater recharge from Scenario 1 to Scenario 3 (Fig. 4). In other words, impacts of precipitation on hydraulic head are larger, when the aquifer is relatively dry with smaller amount of precipitation (or equivalently recharge). The variation pattern of the index (S_{T_K}) of hydraulic conductivity K is opposite. Also for the homogeneous models (R_1Z_1 and R_2Z_1), S_{T_K} decreases from Scenario 1 (wet scenario) to Scenario 3 (dry scenario), because hydraulic conductivity becomes more important when recharge increases so that excessive water from precipitation can be discharged to the constant head boundary (Fig. 1).

For the heterogeneous models (R_1Z_2 and R_2Z_2), Table 1 reveals different variation patterns in the total sensitivity values from Scenario 1 to Scenario 3. It is observed that the importance of precipitation decreases in that S_{T_p} decreases from the range of 67.74–92.98% for the homogeneous models to the range of 5.96–23.75% for the heterogeneous models. Parameter K_2 becomes the most important parameter, which is reasonable because this parameter controls the amount of groundwater flow from the entire modeling domain to the river (Fig. 1). Different from the variation pattern for the homogeneous models, S_{T_p} decreases from Scenario 1 to Scenario 3, because the small parameter value of K_2 blocks the discharge to the river and the precipitation variation determines the precipitation influence on hydraulic head at the location of $x = 6000$ m, recalling that the precipitation variation is larger in Scenario 1 than in Scenario 3 (Fig. 3). This demonstrates again that parameter sensitivity indices change between the individual models and under different scenarios.

Table 1

Total-effect sensitivity index of hydraulic conductivity (S_{T_K} , $S_{T_{K_1}}$ and $S_{T_{K_2}}$) and precipitation (S_{T_p}) calculated for hydraulic head at $x = 6000$ m under four models and three scenarios. The indices for multiple models but individual scenarios are denoted as S_T^M ; the indices for multiple models and multiple scenarios are denoted as S_T^{MS} .

	Scenario 1				Scenario 2				Scenario 3			
	R_1Z_1	R_2Z_1	R_1Z_2	R_2Z_2	R_1Z_1	R_2Z_1	R_1Z_2	R_2Z_2	R_1Z_1	R_2Z_1	R_1Z_2	R_2Z_2
S_{T_p} (%)	67.74	89.33	23.75	22.26	73.60	91.97	18.61	8.90	76.64	92.98	17.03	5.96
S_{T_K} (%)	32.39	10.99	0	0	26.83	8.64	0	0	23.60	7.27	0	0
$S_{T_{K_1}}$ (%)	0	0	3.15	8.58	0	0	5.79	13.70	0	0	6.99	15.33
$S_{T_{K_2}}$ (%)	0	0	73.07	69.18	0	0	75.74	77.47	0	0	76.47	79.16
<i>After model averaging: Total-effect sensitivity index for multiple models but individual scenarios</i>												
$S_{T_p}^M$ (%)		35.78				24.31					21.41	
$S_{T_K}^M$ (%)		5.82				3.59					2.82	
$S_{T_{K_1}}^M$ (%)		4.28				7.79					9.20	
$S_{T_{K_2}}^M$ (%)		54.22				64.33					67.00	
<i>After scenario averaging: Total-effect sensitivity index for multiple models and multiple scenarios</i>												
$S_{T_p}^{MS}$ (%)						28.09						
$S_{T_K}^{MS}$ (%)						4.27						
$S_{T_{K_1}}^{MS}$ (%)						6.77						
$S_{T_{K_2}}^{MS}$ (%)						60.99						

4.2. Total sensitivity index for head under multiple models but individual scenarios

To evaluate the total sensitivity index (S_T^M in Eq. (16)) listed in Table 1 for the four models but three individual scenarios, equal model probability (25%) is assigned to the four models for model averaging. It should be noted that S_T^M of the multiple models is not a weighted average of S_T of the individual models, because model averaging is conducted for the variance, not the index, of the individual models (Eq. (16)). Table 1 demonstrates that the new sensitivity indices can be evaluated when different models have different number of parameters. For example, $S_{T_{K_2}}^M$ is evaluated for parameter K_2 that only belongs to models R_1Z_2 and R_2Z_2 , and $S_{T_P}^M$ is estimated for parameter P that exists for all the four models. The model and scenario averaging techniques make it possible to compare the importance of different parameters which do not coexist in the same models.

The total sensitivity indices, S_T^M , obtained after model averaging indicate that precipitation is the second most influential parameter, although it is the most influential parameter for models R_1Z_1 and R_2Z_1 . This demonstrates that considering multiple models in the calculation of the sensitivity indices helps to prevent biased identification of important parameters based only on a single model. In other words, an important parameter of one model may not be important for multiple models, depending on uncertainty magnitude of the parameter for the individual models.

The most influential parameter is parameter K_2 , and it can be explained by Fig. 5a which plots the PDFs of the simulated hydraulic head by the four models under the three scenarios. The figure shows that, for a given scenario, the head uncertainty of the two-zone models is larger than that of the one-zone models. For parameters K_1 and K_2 of the two-zone models, K_2 is more influential to head simulation than K_1 , because K_2 controls the groundwater flow to the river located at the right hand side of the domain. The high sensitivity values of K_2 and P are useful for evaluating relative plausibility of the models. For example, if head observations are available, they can be used to discriminate between the two recharge models and between the two groundwater flow models.

4.3. Total sensitivity index for head under multiple models and multiple scenarios

For conducting scenario averaging, equal scenario probability (1/3) is assigned to the three scenarios. Table 1 lists the total sensitivity index, S_T^{MS} , of precipitation and hydraulic conductivity for multiple models and multiple scenarios. The sensitivity indices are the final measure of global parameter sensitivity with consideration of the combining effects of parameter, model, and scenario uncertainties. The S_T^{MS} values are similar to the S_T^M values of the individual scenarios, but different from the S_T values of individual models and scenarios. In particular, the S_T values of Model R_1Z_1 and R_2Z_1 under the three scenarios suggests that the precipitation is the most important parameter, while the S_T^{MS} (and S_T^M) values indicate that hydraulic conductivity K_2 is more important. It suggests that, without considering model and scenario uncertainty, it is likely that a biased identification of important parameter may occur.

The reason that the S_T^{MS} values are similar to the S_T^M values is that the head variance after model averaging is similar under the three scenarios, as shown in Fig. 5b. It suggests that scenario uncertainty plays a less important role than model uncertainty in terms of identifying important parameters. This however is not a general case but specific to this synthetic example. The general uncertainty framework (Eq. (8)) and the new sensitivity indices are useful to evaluate relative contributions from different uncertainty sources to predictive uncertainty, and to identify important parameters with consideration of the uncertainty sources.

4.4. Total sensitivity index for ethene concentration

The three sets (S_T , S_T^M , and S_T^{MS}) of total global sensitivity index are evaluated for ethene concentration at the location of $x = 6,000$ m after 1000 days, and their values are listed in Table 2. The table shows again that the sum of the four indices (i.e., S_{T_P} for precipitation, $S_{T_{K_1}}$, $S_{T_{K_2}}$ for hydraulic conductivity, S_{T_D} for dispersion coefficient, and $S_{T_{k_1}}$ for first-order degradation coefficient of PCE) is slightly larger than 1, suggesting that the

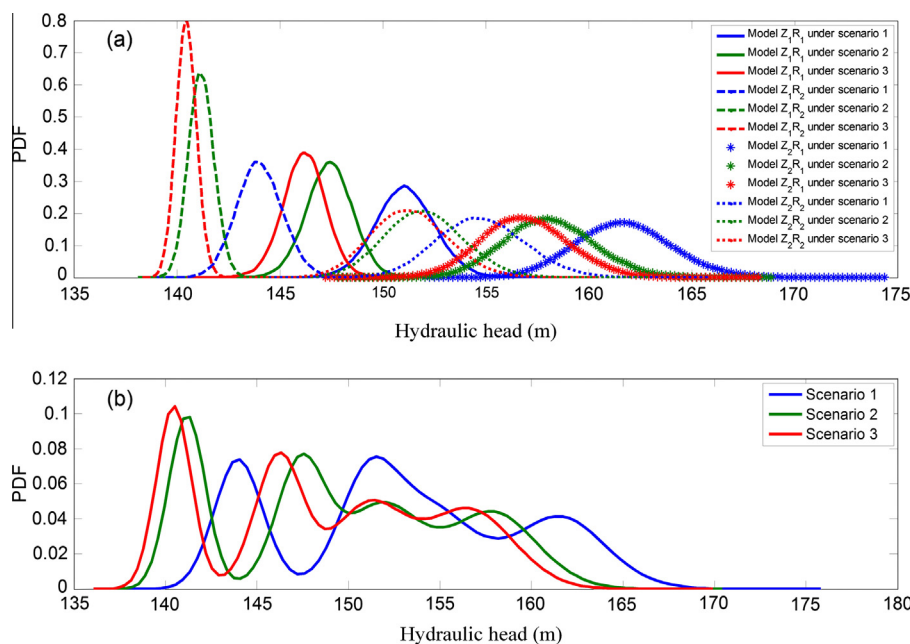


Fig. 5. Probability density functions (PDFs) of hydraulic head at $x = 6000$ m simulated by (a) the two models under the three scenarios and (b) modeling averaging under the three scenarios.

Table 2

Total-effect sensitivity index of model parameters calculated for ethene concentration at $x = 6000$ m under four models and three scenarios.

	Scenario 1				Scenario 2				Scenario 3			
	R ₁ Z ₁	R ₂ Z ₁	R ₁ Z ₂	R ₂ Z ₂	R ₁ Z ₁	R ₂ Z ₁	R ₁ Z ₂	R ₂ Z ₂	R ₁ Z ₁	R ₂ Z ₁	R ₁ Z ₂	R ₂ Z ₂
S_{T_p} (%)	5.19	5.73	0.02	0.06	4.18	2.25	0.03	0.03	4.01	1.54	0.03	0.02
S_{T_K} (%)	94.68	94.12	0	0	95.23	97.19	0	0	95.45	97.92	0	0
$S_{T_{K_1}}$ (%)	0	0	1.97	1.38	0	0	1.81	0.97	0	0	1.30	0.71
$S_{T_{K_2}}$ (%)	0	0	97.99	98.66	0	0	98.36	98.98	0	0	99.05	99.64
S_{T_D} (%)	0.00	0.00	0.00	0.00	0.00	0.00	0.00	0.00	0.00	0.00	0.00	0.00
$S_{T_{K_1}}$ (%)	0.90	0.85	0.13	0.16	0.90	0.74	0.15	0.17	0.90	0.71	0.15	0.17
<i>After model averaging: S_T^M for multiple models but individual scenarios</i>												
$S_{T_p}^M$ (%)	0.37				0.28				0.26			
$S_{T_K}^M$ (%)	5.72				8.49				9.48			
$S_{T_{K_1}}^M$ (%)	1.37				1.02				0.92			
$S_{T_{K_2}}^M$ (%)	92.43				90.36				89.61			
$S_{T_D}^M$ (%)	0.00				0.00				0.00			
$S_{T_{K_1}}^M$ (%)	0.19				0.22				0.23			
<i>After scenario averaging: S_T^{MS} for multiple models and multiple scenarios</i>												
$S_{T_p}^{MS}$ (%)					0.30							
$S_{T_K}^{MS}$ (%)					7.85							
$S_{T_{K_1}}^{MS}$ (%)					1.11							
$S_{T_{K_2}}^{MS}$ (%)					90.63							
$S_{T_D}^{MS}$ (%)					0.00							
$S_{T_{K_1}}^{MS}$ (%)					0.21							

first-order and total sensitivity indices have similar values. Therefore, only the values of total sensitivity index are shown and discussed.

For the individual models and individual scenarios, the most important parameter is hydraulic conductivity (K for the one-zone models and K_2 for the two-zone models), indicating that hydraulic conductivity is the most influential parameters to the concentration simulation in this synthetic case. The S_T values of precipitation are small, ranging from 0.02% to 5.19%, which is reasonable because the variation of hydraulic gradient with precipitation is relatively small. The S_T values of dispersion coefficient are zero, which is attributed to the narrow range (10.0–10.1 m²/d) of the parameter and the one-dimensional flow. The S_T values of degradation coefficient are also negligible, because, for most of the realizations, the plume of ethene (the last product of the chain reaction) has not reached the location of $x = 6000$ m within 1000 days. If S_T is evaluated at another location of $x = 5200$ m where ethene reaches this location after 1000 days for most of realizations, the S_T value of degradation coefficient can be significantly larger, e.g., 19.83% for model R₁Z₁ under Scenario 2. These results of sensitivity analysis suggest that, in the synthetic case, the ethene transport at $x = 6000$ m and within 1000 days is largely affected by the flow parameters. This is reasonable because the dispersive transport is negligible and advective transport is controlled jointly by hydraulic conductivity and precipitation.

The S_T^M and S_T^{MS} values listed in Table 2 indicate that hydraulic conductivity (K for the one-zone models and K_2 for the two-zone models) is still the most important parameters after the model and scenario averaging. However, the $S_{T_K}^M$ values become dramatically smaller than the S_{T_K} values of the individual models, while the $S_{T_{K_2}}^M$ values are similar to the $S_{T_{K_2}}$ values of the individual models. This leads to a conclusion that K_2 is significantly more important than K , which is consistent with the results listed in Table 1 for the sensitivity of hydraulic head to hydraulic conductivity. The values of S_T^{MS} are similar to the values of S_T^M under the

individual scenarios, suggesting again that scenario uncertainty is less important than model uncertainty to ethene concentration at $x = 6000$ m after 1000 days. In this sense, identification of important parameters based on a single scenario is not biased. This however is unknown until the S_T , S_T^M , and S_T^{MS} values are evaluated.

4.5. Impacts of model and scenario probabilities on total sensitivity index

All the results above are based on equal model probability, $P(M|S) = 1/4$, and equal scenario probability, $P(S) = 1/3$. This section investigates the impact of model and scenario probabilities on the global sensitivity indices by evaluating the indices using multiple sets of model and scenario probabilities. Following Ye et al. (2005), the minimum and maximum probabilities of a single model are set as 5% and 85%, respectively, and the probability increment is 5%. This leads to 969 sets of model probability, considering that four models are considered in this study. In the same manner, 172 sets of scenario probabilities are obtained for the three scenarios. We here only present the results of impact analysis conducted for precipitation based on the hydraulic head simulations at $x = 6000$ m; the parameter of precipitation is selected because it exists for all the four models.

Fig. 6 plots the maximum and minimum values of $S_{T_p}^M$ for hydraulic head at $x = 6000$ m under Scenario 1 with the probability of Model R₁Z₁. The maximum and minimum values are selected from the $S_{T_p}^M$ values evaluated using the 969 sets of model probabilities for the four models. The figure demonstrates that $S_{T_p}^M$ value is dramatically affected by the model probabilities. The value of $S_{T_p}^M$ can vary from 31.19% to 73.31%, when Model R₁Z₁ has the probability of 5%. When the probability of Model R₁Z₁ increases from 5% to 85%, the range of $S_{T_p}^M$ values decreases monotonically from 42.12% to 0. The reason is that the number of combinations of model probability decreases from 153 (when the probability of

R_1Z_1 is 5%) to 1 (when the probability of R_1Z_1 is 85%). In addition, the S_T values vary substantially between the models. The monotonic increase (decrease) of the minimum (maximum) value of $S_{T_p}^M$ is not surprising, because the sensitivity index is the portion of variance of the individual model to the averaged variance. It is therefore important to use accurate model probability for model averaging. While the prior weights are used in this study, the posterior weights can be used for calculating the sensitivity indices when observations are available (see the review article of Schoniger et al., 2014).

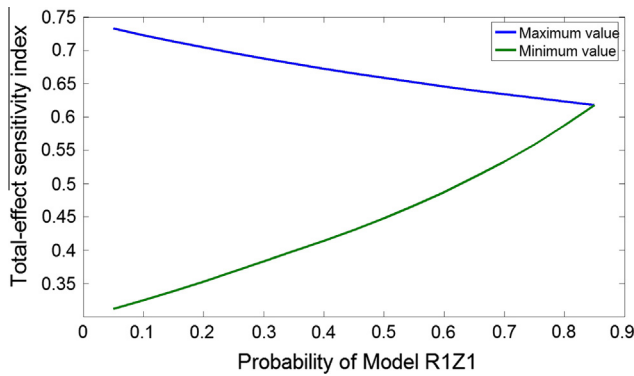


Fig. 6. Maximum and minimum of total-effect sensitivity index ($S_{T_p}^M$, after model averaging) of precipitation for hydraulic head at $x = 6000$ m under scenario 1 with changing model probabilities. The probability of Model R_1Z_1 varies between 5% and 85%.

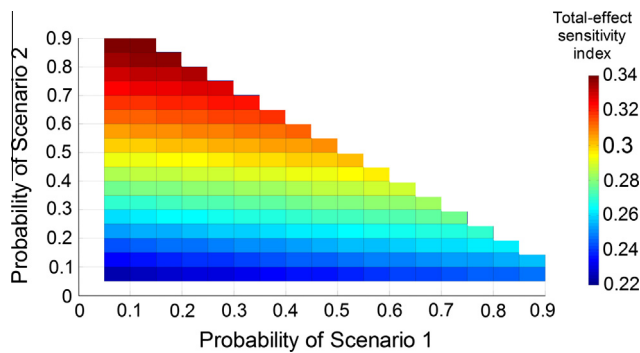


Fig. 7. Total-effect sensitivity index ($S_{T_p}^{MS}$, after scenario averaging) of precipitation for hydraulic head at $x = 6000$ m evaluated using multiple sets of scenario probabilities.

Fig. 7 plots the $S_{T_p}^{MS}$ values of precipitation with the 172 probability sets of Scenarios 1–3. Because the focus is to evaluate the impacts of scenario uncertainty, equal model probability is used for the evaluation of $S_{T_p}^{MS}$. The upper part of the figure is blank, where the requirement of $\sum_s P(S) = 1$ is not satisfied for the scenario probabilities. Fig. 7 shows that, in comparison with the large impacts of model probabilities on $S_{T_p}^M$, the impact of scenario probabilities on $S_{T_p}^{MS}$ is relatively small, as reflected by the small variation of $S_{T_p}^{MS}$ with the scenario probabilities. This may be explained by the small difference of $S_{T_p}^M$ between the three scenarios (Fig. 5 and Table 1). In other words, the impact of scenario probabilities on $S_{T_p}^{MS}$ is insignificant because of relatively small variation of $S_{T_p}^M$ between the scenarios. Therefore, the impact of model and scenario probability on the sensitivity indices are secondary in comparison with the variability of the indices between models and/or scenarios.

4.6. Accuracy of sparse grid collocation algorithm

All the results above are based on 1,000,000 MC simulations using the quasi-random sampling method of Saltelli et al. (2010). The results are used as the yardstick to evaluate the accuracy of the SGC algorithm described in Section 2.3. The Gauss-Hermite and Clenshaw-Curtis rules are used for the normal and uniform distributions, respectively. The SGC precision levels l_1 – l_6 described in Section 2.3 are chosen to be the same value, ranging from 1 to 3 for the flow modeling and from 1 to 4 for the transport modeling. This reduces the number of sparse grids from six to two, which are $I_1 = I_4$ for θ_{-i} and $I_2 = I_3 = I_5 = I_6$ for θ_i . In this way, the number of sparse grid points is reduced from $m_1m_2 + m_1m_3 + m_4m_5 + m_4m_6$ to m_1m_2 . Table 3 lists the total sensitivity values of precipitation (S_{T_p}) and hydraulic conductivity (S_{T_k}) evaluated for hydraulic head and ethene concentration of Model R_1Z_1 under Scenario 2. The S_T values are evaluated for different numbers of MC samples (NMCS) and different numbers of SG points (NSGP). In addition, the numbers of model executions (NME) are also listed. For the quasi-random sampling method, as discussed in Section 2.3, $NME = (2 + d)n$, where d is number of parameters and n is number of samples. For the SGC method, NSGP and NME depend on precision levels (l) and number of parameters (d). For example, to evaluate NSGP for evaluating S_{T_k} of ethene concentration, if the precision levels are set as $l_4 = 1$ and $l_5 = 1$, NSGP is 21 and NME is 84, because the sparse grid calculation needs to be repeated for each of the four

Table 3
Number of Monte Carlo samples (NMCS) and number of model executions (NME) of quasi-random sampling method used to calculate total-effect global sensitivity index for hydraulic head and ethene concentration of model R_1Z_1 under scenario 2. The number of sparse grid points (NSGP) for different levels of precision, and corresponding NME are also listed to show that NME is dramatically reduced in the sparse grid collocation method.

NMCS	NME	S_{T_k}	S_{T_p}	NSGP	Level	NME	S_{T_k}	S_{T_p}
For hydraulic head at $x = 6000$ m								
50	200	0.160	0.640	9	1	18	0.325	0.791
100	400	0.240	0.878	25	2	50	0.268	0.735
1000	4000	0.265	0.767	49	3	98	0.268	0.735
10,000	40,000	0.251	0.732					
100,000	400,000	0.269	0.735					
1,000,000	4,000,000	0.268	0.735					
For ethene concentration at $x = 6000$ m and on 1000 days								
50	300	0.700	0.052	21	1	84	0.900	-0.047
100	600	1.105	0.043	145	2	590	0.947	0.035
1000	6000	0.849	0.039	651	3	2898	0.951	0.040
10,000	60,000	0.959	0.043	2277	4	11,880	0.952	0.042
100,000	600,000	0.960	0.043					
1,000,000	6,000,000	0.952	0.042					

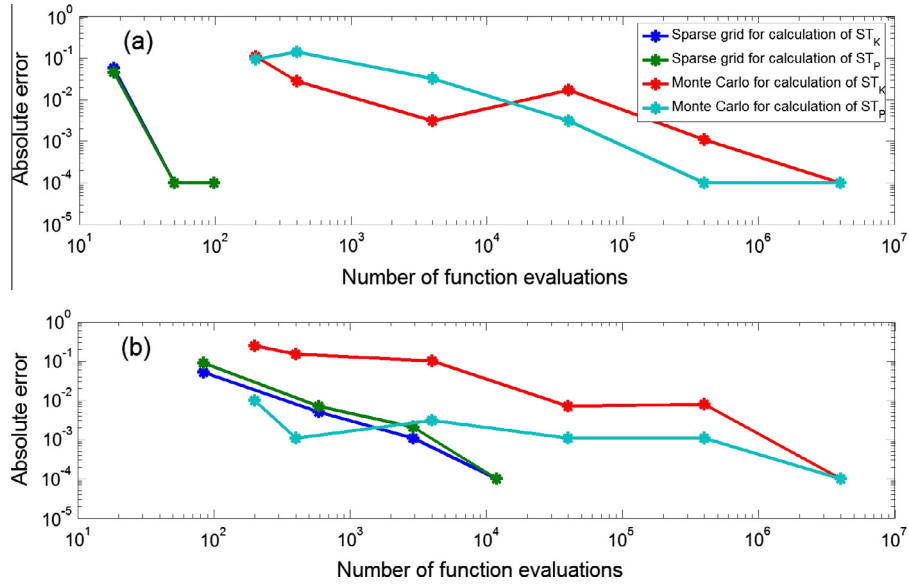


Fig. 8. Absolute error plotted with the function evaluation numbers for the total-effect sensitivity indices of (a) hydraulic head and (b) ethene concentration at $x = 6000$ m using SGC and MC methods.

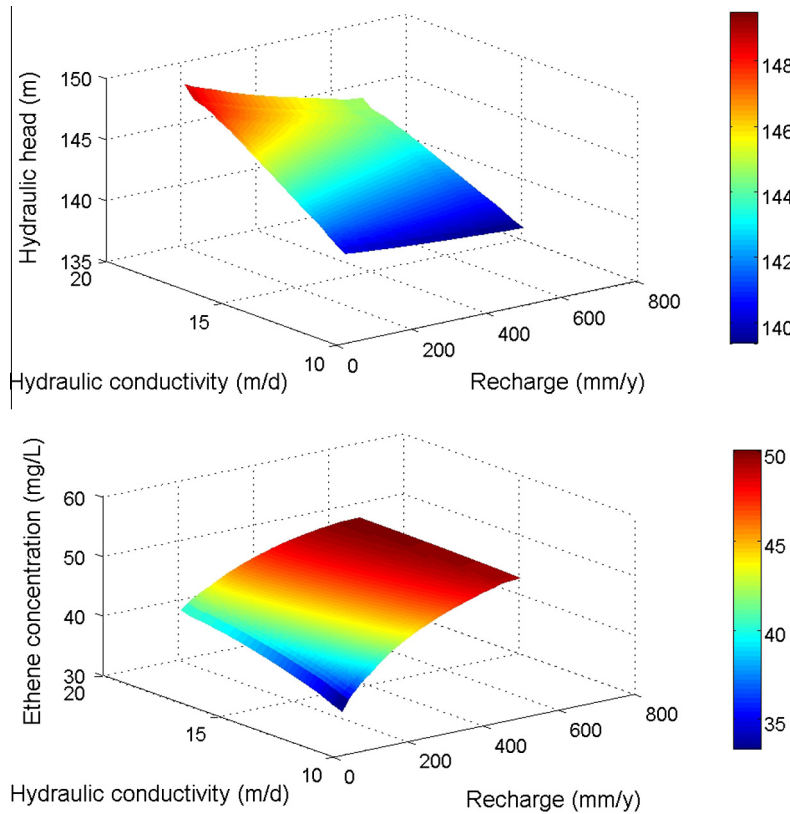


Fig. 9. (a) Hydraulic head and (b) ethene concentration at $x = 6000$ m in the parameter space of hydraulic conductivity and groundwater recharge.

parameters. NSGP is significantly larger for the transport modeling than for the flow modeling, because the transport modeling involves four parameters but the flow modeling only involves two parameters.

Table 3 shows that the SGC algorithm can dramatically save computational cost in comparison with the quasi-random sampling method. For the flow modeling, only 50 model executions (with 25 SGP) are needed to achieve the same results obtained

from four million model executions (with one million samples). For the transport modeling, the SGC computational cost increases, and 11,880 model executions (with 2,277 SGP) are needed, which is still significantly more efficient than the quasi-random sampling method. While one million samples may not be absolutely needed for the quasi-random sampling method, at least 100,000 samples are needed due to the well-known slow convergence of MC simulation.

To investigate the accuracy and convergence rate of the quasi-random sampling method and the SGC method, Fig. 8 plots the absolute errors of the total sensitivity index with number of function evaluations calculated for the head and ethene concentration of Model R₁Z₁ and Scenario 2. The reference values used for calculating the errors are obtained from 2,000,000 MC simulations (8,000,000 of model executions) of the quasi-random sampling method. While the final errors of the two methods are as small as $\sim 10^{-4}$, the figure demonstrates that the convergence rate of the SGC method is significantly faster than that of the MC method. The SGC converge rate for hydraulic head is faster than that for the ethene concentration, which is attributed to the relatively smaller parameter number and smoother function for hydraulic head (Fig. 9).

The computational saving of the SGC method is attributed to the relatively small number of model parameters and the smoothness of hydraulic head and ethene concentration in the parameter space, as shown in Fig. (9). When the number of model parameters increase, the number of SG points increases accordingly to yield accurate SG integration (Table 3 and Fig. 8). This however should not be a barrier to the applications of the SGC algorithm, because it has been shown to be computationally efficient to resolve the problem of the curse of dimensionality in the literature of applied mathematics (Bungartz and Griebel, 2004; Gerstner and Griebel, 1998; Nobile et al., 2008). On the other hand, when smoothness of a function deteriorates, more SG points are needed to yield accurate SG integration. As shown in Fig. 9, both the head and concentration surfaces are smooth in the parameter space of the synthetic case. It should be noted that function smoothness and nonlinearity are two different concepts. In other words, the SGC algorithm can be sufficiently efficient for a nonlinear model if its output is smooth. Special techniques are necessary for a non-smooth function. For example, Zhang et al. (2013a, 2013b) used optimization to identify high-probability regions before SGC surrogate was built, and adaptive SGC was used for the high probability regions to save computational cost. More research is warranted for applying SGC to highly non-smooth functions.

5. Conclusions

To tackle the problem that conventional variance-based global sensitivity analysis considers only parametric uncertainty, this paper defines new global sensitivity indices with consideration of parameter, model, and scenario uncertainties. With the hierarchical framework of uncertainty quantification, the first-order (S) and total-effect (S_T) sensitivity indices are defined for the three situations: (1) a single model and a single scenario, (2) multiple models but a single scenario, and (3) multiple models and multiple scenarios. The definition of the first situation is the same as the conventional one; the indices of the second situation (denoted as S^M and S_T^M) are new to address model uncertainty by using a model-averaging method. Similarly, the new indices of the third situation (denoted as S^{MS} and S_T^{MS}) take into account of both model and scenario uncertainties by using model- and scenario-averaging methods. It should be noted that S^M and S_T^M are not simply model averaging of S and S_T , respectively, and S^{MS} and S_T^{MS} are not simply scenario averaging of S^M and S_T^M , respectively. Since S and S_T may vary significantly between alternative models and/or alternative scenarios, using the new indices can avoid biased identification of important parameters. This is demonstrated in the numerical example of groundwater flow and reactive transport modeling, which considers three scenarios of precipitation, four alternative models with different conceptualizations of parameterization and

recharge components, and six random model parameters. The numerical example also shows that model and scenario probabilities have significant impacts on the index values, especially when the values vary substantially between alternative models and alternative scenarios.

To resolve the problem that global sensitivity analysis is computationally expensive, a computationally efficient sparse grid collocation method (SGC) is used. Instead of relying on computationally demanding MC methods, the mean and variance terms involved in the global sensitivity analysis are evaluated directly using the sparse grid integration techniques. The SGC method is flexible to allow using different sparse grids for different mean and variance terms and using different quadrature rules for different parameter distributions. The SGC results are accurate, in comparison with those obtained using the popular quasi-random sampling method. The computational cost is dramatically reduced. For the numerical example, the SGC only needs hundreds and tens of hundreds of model execution to yield the same results as the quasi-random sampling method that requires hundreds of thousands and millions of model executions.

While the new framework of global sensitivity analysis is theoretically general and numerically easy to implement, applications of the method heavily depend on the model and scenario averaging weights. While the new sensitivity indices can be evaluated using either prior or posterior model averaging weights, obtaining the weights is still an open research area. When the priors are used, it is challenging to elicit the priors due to the subjective nature of priors, as discussed in O'Hagan and Oakley (2004) and Ye et al. (2008b). When the posteriors are used, MC methods that are necessary for estimating the posteriors are computationally expensive. The computational burden may be alleviated by using sparse grid collocation modeling to build surrogates of models or model likelihoods, as shown in Zhang et al. (2013a, 2013b). However, computational efficiency of sparse grid methods may deteriorate when the number of model parameters. In addition, when the model outputs or functions of the outputs is highly non-smooth (Shi et al., 2014 showed a highly non-smoothed likelihood function for a groundwater reactive transport model), the sparse grid methods may not perform well until a large number of sparse grid points are used (Ganapathysubramanian and Zabarar, 2007; Ma and Zabarar, 2009). It is expected that these problems can be resolved when more advanced numerical methods are developed in the future.

Acknowledgments

This work was supported in part by the DOE Early Career Award DE-SC0008272. We thank John Burkardt for helping on sparse grid collocation, Yunwei Sun on analytical solution of multispecies reactive transport modeling, and Wolfgang Nowak and Anneli Schoniger for handling and reviewing the manuscript.

Appendix A. Variance decomposition

Using the law of total variance and considering uncertain scenarios in a set, \mathbf{S} , of multiple scenarios, S , variance of Δ can be decomposed as

$$V(\Delta) = E_S V(\Delta|\mathbf{S}) + V_S E(\Delta|\mathbf{S}). \quad (\text{A1})$$

The first and the second term at the right hand side of the equation are termed by Draper et al. (1999) as within-scenario variance and between-scenario variance, respectively. Considering a set, \mathbf{M} , of multiple models, M , decompose $V(\Delta|\mathbf{S})$ as

$$V(\Delta|\mathbf{S}) = E_{\mathbf{M}|\mathbf{S}}V(\Delta|\mathbf{M}, \mathbf{S}) + V_{\mathbf{M}|\mathbf{S}}E(\Delta|\mathbf{M}, \mathbf{S}) \quad (\text{A2})$$

The first and second term at the right hand side of the equations are termed as within-model variance and between-model variance, respectively (Draper, 1995; Hoeting et al., 1999). Substituting (A2) into (A1) and applying the law of total expectation to the latter term at the right hand side of (A1) leads to:

$$\begin{aligned} V(\Delta) &= E_{\mathbf{S}}(E_{\mathbf{M}|\mathbf{S}}V(\Delta|\mathbf{M}, \mathbf{S}) + V_{\mathbf{M}|\mathbf{S}}E(\Delta|\mathbf{M}, \mathbf{S})) + V_{\mathbf{S}}E_{\mathbf{M}|\mathbf{S}}E(\Delta|\mathbf{M}, \mathbf{S}) \\ &= E_{\mathbf{S}}E_{\mathbf{M}|\mathbf{S}}V(\Delta|\mathbf{M}, \mathbf{S}) + E_{\mathbf{S}}V_{\mathbf{M}|\mathbf{S}}E(\Delta|\mathbf{M}, \mathbf{S}) + V_{\mathbf{S}}E_{\mathbf{M}|\mathbf{S}}E(\Delta|\mathbf{M}, \mathbf{S}) \end{aligned} \quad (\text{A3})$$

Considering uncertainty in model parameters θ , decompose $V(\Delta|\mathbf{M}, \mathbf{S})$ as

$$V(\Delta|\mathbf{M}, \mathbf{S}) = E_{\theta|\mathbf{M}, \mathbf{S}}V(\Delta|\theta, \mathbf{M}, \mathbf{S}) + V_{\theta|\mathbf{M}, \mathbf{S}}E(\Delta|\theta, \mathbf{M}, \mathbf{S}) \quad (\text{A4})$$

Substituting (A4) into (A3) and applying the law of total expectation to the latter two terms at the right hand side of (A3) gives

$$\begin{aligned} V(\Delta) &= E_{\mathbf{S}}E_{\mathbf{M}|\mathbf{S}}(E_{\theta|\mathbf{M}, \mathbf{S}}V(\Delta|\theta, \mathbf{M}, \mathbf{S}) + V_{\theta|\mathbf{M}, \mathbf{S}}E(\Delta|\theta, \mathbf{M}, \mathbf{S})) \\ &\quad + E_{\mathbf{S}}V_{\mathbf{M}|\mathbf{S}}E(\Delta|\mathbf{M}, \mathbf{S}) + V_{\mathbf{S}}E_{\mathbf{M}|\mathbf{S}}E(\Delta|\mathbf{M}, \mathbf{S}) \\ &= E_{\mathbf{S}}E_{\mathbf{M}|\mathbf{S}}E_{\theta|\mathbf{M}, \mathbf{S}}V(\Delta|\theta, \mathbf{M}, \mathbf{S}) + E_{\mathbf{S}}E_{\mathbf{M}|\mathbf{S}}V_{\theta|\mathbf{M}, \mathbf{S}}E(\Delta|\theta, \mathbf{M}, \mathbf{S}) \\ &\quad + E_{\mathbf{S}}V_{\mathbf{M}|\mathbf{S}}E_{\theta|\mathbf{M}, \mathbf{S}}E(\Delta|\theta, \mathbf{M}, \mathbf{S}) + V_{\mathbf{S}}E_{\mathbf{M}|\mathbf{S}}E_{\theta|\mathbf{M}, \mathbf{S}}E(\Delta|\theta, \mathbf{M}, \mathbf{S}) \end{aligned} \quad (\text{A5})$$

which is Eq. (8) in the text.

References

- Ajami, N.K., Duan, Q., Sorooshian, S., 2007. An integrated hydrologic Bayesian multimodel combination framework: confronting input, parameter, and model structural uncertainty in hydrologic prediction. *Water Resour. Res.* 43.
- Aziz, C.E., Newell, C.J., Gonzales, J.R., Haas, P.E., Clement, T.P., Sun, Y., 2000. BIOCHLOR Natural Attenuation Decision Support System: User's Manual, Version 1.0. U.S. EPA Office of Research and Development, Washington, DC.
- Baroni, G., Tarantola, S., 2014. A general probabilistic framework for uncertainty and global sensitivity analysis of deterministic models: a hydrological case study. *Environ. Modell. Softw.* 51, 26–34.
- Barthelmann, V., Novak, E., Ritter, K., 1999. High dimensional polynomial interpolation on sparse grid. *Adv. Comput. Math.* 12, 273–288.
- Beven, K., 2002. Towards a coherent philosophy for modeling the environment. *Proc. Roy. Soc. Lond. Ser. A Math. Phys. Eng. Sci.* 458 (2026), 2465–2484.
- Beven, K., 2006. A manifesto for the equifinality thesis. *J. Hydrol.* 320, 18–36.
- Borgonovo, E., Castaigne, W., Tarantola, S., 2012. Model emulation and moment-independent sensitivity analysis: an application to environmental modelling. *Environ. Modell. Softw.* 34, 105–115.
- Bredheoht, J.D., 2003. From models to performance assessment: the conceptualization problem. *Ground Water* 41 (5), 571–577.
- Bredheoht, J.D., 2005. The conceptualization model problem-surprise. *Hydrogeol. J.* 13, 37–46.
- Bungartz, H.J., Griebel, M., 2004. Sparse grids. *Acta Numer.* 13, 147–269.
- Buzzard, G.T., Xiu, D., 2011. Variance-based global sensitivity analysis via sparse grid interpolation and cubature. *Commun. Comput. Phys.* 9, 542–567.
- Buzzard, G.T., 2012. Global sensitivity analysis using sparse grid interpolation and polynomial chaos. *Rel. Eng. Syst. Saf.* 107, 82–89.
- Chen, X., Ng, B.M., Sun, Y., Tong, C.H., 2013. A computational method for simulating subsurface flow and reactive transport in heterogeneous porous media embedded with flexible uncertainty quantification. *Water Resour. Res.* 49, 5740–5755. <http://dx.doi.org/10.1002/wrcr.20454>.
- Chu-Agor, M.L., Muñoz-Carpena, R., Kiker, G., Emanuelsson, A., Linkov, I., 2011. Exploring sea level rise vulnerability of coastal habitats through global sensitivity and uncertainty analysis. *Env. Model. Software* 26 (5), 593–604. <http://dx.doi.org/10.1016/j.envsoft.2010.12.003>.
- Davis, P.J., Rabinowitz, P., 1975. *Methods of Numerical Integration*. Academic, New York, pp. 67–68.
- Davis, P.J., Rabinowitz, P., 1967. *Numerical Integration*. Blaisdell Pub. Co., Waltham, Massachusetts, pp. 96.
- Draper, D., 1995. Assessment and propagation of model uncertainty. *J. Roy. Stat. Soc. Ser. B* 57 (1), 45–97.
- Draper, D., Pereira, A., Prado, P., Saltelli, A., Cheal, R., Eguilior, S., Mendes, B., Tarantola, S., 1999. Scenario and parametric uncertainty in GESAMAC: A methodological study in nuclear waste disposal risk assessment. *Comput. Phys. Commun.* 117, 142–155.
- Fetter, C.W., 2001. *Applied Hydrogeology*, fourth ed. Prentice-Hall, New Jersey, pp. 143.
- Foglia, L., Mehl, S.W., Hill, M.C., Burlando, P., 2013. Evaluating model structure adequacy: the case of the Maggia Valley groundwater system, southern Switzerland. *Water Resour. Res.* 49. <http://dx.doi.org/10.1029/2011WR011779>.
- Formaggia, L., Guadagnini, A., Imperiali, I., Lever, V., Porta, G., Riva, M., Scotti, A., Tamellini, L., 2013. Global sensitivity analysis through polynomial chaos expansion of a basin-scale geochemical compaction model. *Comput. Geosci.* 17, 25–42. <http://dx.doi.org/10.1007/s10596-012-9311-5>.
- Ganapathysubramanian, B., Zabarar, N., 2007. Sparse grid collocation methods for stochastic natural convection problems. *J. Comput. Phys.* 225 (1), 652–685.
- Garcia-Cabrejo, O., Valocchi, A., 2014. Global sensitivity analysis for multivariate output using polynomial chaos expansion. *Reliab. Eng. Syst. Saf.* 126, 25–36.
- Gerstner, T., Griebel, M., 1998. Numerical integration using sparse grid. *Numer. Algorithms* 18, 209–232.
- Gupta, H.V., Clark, M.P., Vrugt, J.A., Abramowitz, G., Ye, M., 2012. Towards a comprehensive assessment of model structural adequacy. *Water Resour. Res.* 48, W08301. <http://dx.doi.org/10.1029/2011WR011044>.
- Hakami, A., Odman, M.T., Russell, A.G., 2003. High-order direct sensitivity analysis of multidimensional air quality models. *Environ. Sci. Technol.* 37, 2442–2452.
- Helton, J.C., 1993. Uncertainty and sensitivity analysis techniques for use in performance assessment for radioactive waste disposal. *Reliab. Eng. Syst. Saf.* 42, 327–367.
- Helton, J.C., Davis, F.J., 2003. Latin hypercube sampling and the propagation of uncertainty in analyses of complex system. *Reliab. Eng. Syst. Saf.* 81, 23–69.
- Herman, J.D., Reed, P.M., Wagener, T., 2013. Time-varying sensitivity analysis clarifies the effects of watershed model formulation on model behavior. *Water Resour. Res.* 49, 1400–1414.
- Hoeting, J.A., Madigan, D., Raftery, A.E., Volinsky, C.T., 1999. Bayesian model averaging: a tutorial. *Stat. Sci.* 14 (4), 382–417.
- Homma, T., Saltelli, A., 1996. Importance measures in global sensitivity analysis of model output. *Reliab. Eng. Syst. Saf.* 52 (1), 1–17.
- IPCC, 2000. In: Nakicenovic, Nebojsa, Swart, Rob (Eds.), *IPCC Special Report: Emissions Scenarios*. Cambridge University Press, UK.
- Jansen, M.J.M., 1999. Analysis of variance designs for model output. *Comput. Phys. Commun.* 117, 35–43.
- Kavetski, D., Kuczera, G., Franks, S.W., 2006. Bayesian analysis of input uncertainty in hydrological modeling: 1. Theory. *Water Resour. Res.* 42, W03407. <http://dx.doi.org/10.1029/2005WR004368>.
- Kleijnen, J.P.C., 2009. Kriging metamodeling in simulation: a review. *Eur. J. Oper. Res.* 192, 707–716.
- Krishna, R.K., 1987. *Groundwater assessment, development and management*. Tata McGraw-Hill Publishing Co., Ltd., New Delhi, pp. 576–657.
- Lamoureaux, B., Mechbal, N., Masse, J.-R., 2014. A combined sensitivity analysis and Kriging surrogate modeling for early validation of health indicators. *Reliab. Eng. Syst. Saf.* 130, 12–26.
- Lin, G., Tartakovsky, A.M., 2009. An efficient, high-order probabilistic collocation method on sparse grids for three-dimensional flow and solute transport in randomly heterogeneous porous media. *Adv. Water Resour.* 32 (5), 712–722. [10.1016/j.advwatres.2008.09.003](http://dx.doi.org/10.1016/j.advwatres.2008.09.003).
- Lin, G., Tartakovsky, A.M., 2010. Numerical studies of three-dimensional stochastic Darcy's equation and stochastic advection–diffusion–dispersion equation. *J. Sci. Comput.* 43, 92–117. <http://dx.doi.org/10.1007/s10915-010-9346-5>.
- Lin, G., Tartakovsky, A.M., Tartakovsky, D.M., 2010. Uncertainty quantification via random domain decomposition and probabilistic collocation on sparse grids. *J. Comput. Phys.* 229 (19), 6995–7012. <http://dx.doi.org/10.1016/j.jcp.2010.05.036>.
- Lu, D., Ye, M., Neuman, S.P., 2011. Dependence of Bayesian model selection criteria and Fisher information matrix on sample size. *Math. Geosci.* 43 (8), 971–993. <http://dx.doi.org/10.1007/s11004-011-9359-0>.
- Lu, D., Ye, M., Neuman, S.P., Xue, L., 2012. Multimodel Bayesian analysis of data-warehouse applied to unsaturated fractured tuffs. *Adv. Water Resour.* 35, 69–82. <http://dx.doi.org/10.1016/j.advwatres.2011.10.007>.
- Lu, D., Ye, M., Meyer, P.D., Curtis, G.P., Shi, X., Niu, X., Yabusaki, S.B., 2013. Effects of error covariance structure on estimation of model averaging weights and predictive performance. *Water Resour. Res.* 49. <http://dx.doi.org/10.1002/wrcr.20441>.
- Lu, D., Ye, M., Hill, M.C., Poeter, E.P., Curtis, G.P., 2014. Integration of Markov chain Monte Carlo simulation into UCODE for Bayesian uncertainty analysis. *Environ. Model. Software* 60, 45–56. <http://dx.doi.org/10.1016/j.envsoft.2014.06.002>.
- Ma, X., Zabarar, N., 2009. An adaptive hierarchical sparse grid collocation algorithm for the solution of stochastic differential equations. *J. Comput. Phys.* 228, 3084–3113.
- Massmann, C., Holzmann, H., 2012. Analysis of the behavior of a rainfall-runoff model using three global sensitivity analysis methods evaluated at different temporal scales. *J. Hydrol.* 475, 97–110.
- Matott, L.S., Babendreier, J.E., Purucker, S.T., 2009. Evaluating uncertainty in integrated environmental models: a review of concepts and tools. *Water Resour. Res.* 45, W06421. <http://dx.doi.org/10.1029/2008WR007301>.
- Meyer, P.D., Ye, M., Nicholson, T., Neuman, S.P., Rockhold, M., 2014. Incorporating scenario uncertainty within a hydrogeologic uncertainty assessment methodology. In: Mosleh, Ali, Jeffery, Wood (Eds.), *Proceedings of the International Workshop on Model Uncertainty: Conceptual and Practical Issues in the Context of Risk-Informed Decision Making*. International Workshop Series on Advanced Topics in Reliability and Risk Analysis, Center for Risk and Reliability, University of Maryland, College Park, MD, USA, 2014, pp. 99–119 (ISSN: 1084-5658).
- Meyer, P.D., Ye, M., Rockhold, M.L., Neuman, S.P., Cantrell, K.J., 2007. Combined Estimation of Hydrogeologic Conceptual Model, Parameter, and Scenario Uncertainty with Application to Uranium Transport at the Hanford Site 300 area. *NUREG/CR-6940 (PNNL-16396)*. U.S. Nuclear Regulatory Commission, Washington, DC.
- Mishra, S., Deeds, N., Ruskauff, G., 2009. Global sensitivity analysis techniques for probabilistic ground water modeling. *Ground Water* 47, 727–744.

- Morris, M.D., 1991. Factorial sampling plans for preliminary computational experiments. *Technometrics* 33 (2), 161–174.
- Neuman, S.P., 2003. Maximum likelihood Bayesian averaging of alternative conceptual-mathematical models. *Stoch. Env. Res. Risk* 17 (5), 291–305. <http://dx.doi.org/10.1007/s00477-003-0151-7>.
- Neuman, S.P., Xue, L., Ye, M., Lu, D., 2012. Bayesian analysis of data-worth considering model and parameter uncertainties. *Adv. Water Resour.* 36, 75–85. <http://dx.doi.org/10.1016/j.advwatres.2011.02.007>.
- Nobile, F., Tempone, R., Webster, C.G., 2008. A sparse grid stochastic collocation method for partial differential equations with random input data. *SIAM J. Numer. Anal.* 46, 2309–2345.
- Nossent, J., Elsen, P., Bauwens, W., 2011. Sobol' sensitivity analysis of a complex environmental model. *Environ. Modell. Softw.* 26, 1515–1525.
- Novak, E., Ritter, K., 1999. Simple cubature formulas with high polynomial exactness. *Constr. Approx.* 15, 499–522.
- O'Hagan, A., Oakley, J.E., 2004. Probability is perfect, but we can't elicit it perfectly. *Reliab. Eng. Syst. Saf.* 85, 239–248.
- O'Hagan, A., 2006. Bayesian analysis of computer code outputs: A tutorial. *Reliab. Eng. Syst. Saf.* 91, 1290–1300.
- Oladyshkin, S., de Barros, F.P.J., Nowak, W., 2012. Global sensitivity analysis: a flexible and efficient framework with an example from stochastic hydrogeology. *Adv. Water Resour.* 37, 10–22.
- Pan, F., Zhu, J., Ye, M., Pachepsky, Y.A., Wu, Y.-S., 2011. Sensitivity analysis of unsaturated flow and contaminant transport with correlated parameters. *J. Hydrol.* 397, 238–249. <http://dx.doi.org/10.1016/j.jhydrol.2010.11.045>.
- Poeter, E.P., Anderson, D.A., 2005. Multimodel ranking and inference in ground water modeling. *Ground Water* 43 (4), 597–605.
- Rakovec, O., Hill, M.C., Clark, M.P., Weerts, A.H., Teuling, A.J., Uijlenhoet, R., 2014. Distributed Evaluation of Local Sensitivity Analysis (DELSA), with application to hydrologic models. *Water Resour. Res.* 50, 409–426. <http://dx.doi.org/10.1002/2013WR014063>.
- Rasmussen, C.E., Williams, C.K.I., 2006. *Gaussian Processes for Machine Learning*. MIT Press, Cambridge, MA.
- Razavi, S., Tolson, B.A., Burn, D.H., 2012. Review of surrogate modeling in water resources. *Water Resour. Res.* 48, W07401. <http://dx.doi.org/10.1029/2011WR011527>.
- Rosolem, R., Gupta, H.V., Shuttleworth, W.J., Zeng, X., de Gonçalves, L.G.G., 2012. A fully multiple-criteria implementation of the Sobol' method for parameter sensitivity analysis. *J. Geophys. Res.* 117, D07103. <http://dx.doi.org/10.1029/2011JD016355>.
- Refsgaard, J.C., Christensen, S., Sonnenborg, T.O., Seifert, D., Hojberg, A.L., Trolborg, L., 2012. Review of strategies for handling geological uncertainty in groundwater flow and transport modeling. *Adv. Water Resour.* 36, 36–50.
- Rojas, R., Kahunde, S., Peeters, L., Batelaan, O., Feyen, L., Dassargues, A., 2010. Application of a multimodel approach to account for conceptual model and scenario uncertainties in groundwater modelling. *J. Hydrol.* 394 (3–4), 416–435.
- Renard, B., Kavetski, D., Kuczera, G., Thyer, M., Franks, S.W., 2010. Understanding predictive uncertainty in hydrologic modeling: The challenge of identifying input and structural errors. *Water Resour. Res.* 46, W05521. <http://dx.doi.org/10.1029/2009WR008328>.
- Saltelli, A., 2000. What is sensitivity analysis? In: Saltelli, A., Chan, K., Scott, M. (Eds.), *Sensitivity analysis*. Wiley, Chichester, pp. 3–14.
- Saltelli, A., Sobol, I.M., 1995. About the use of rank transformation in sensitivity analysis of model output. *Reliab. Eng. & Syst. Safe.* 50 (3), 225–239.
- Saltelli, A., Tarantola, S., Chan, K.P.-S., 1999. A quantitative model independent method for global sensitivity analysis of model output. *Technometrics* 41, 39–56.
- Saltelli, A., Tarantola, S., Chan, K., 1998. Presenting results from model based studies to decision makers: can sensitivity analysis be a defogging agent? *Risk Anal.* 18, 799–803.
- Saltelli, A., Annoni, P., Azzini, I., Campolongo, F., Ratto, M., Tarantola, S., 2010. Variance based sensitivity analysis of model output. Design and estimator for the total sensitivity index. *Comput. Phys. Commun.* 181 (2), 259–270.
- Scanlon, B.R., Healy, R.W., Cook, P.G., 2002. Choosing appropriate techniques for quantifying groundwater recharge. *Hydrogeol. J.* 10, 18–39.
- Schoniger, A., Wholing, T., Samaniego, L., Nowak, W., 2014. Model selection on solid ground: rigorous comparison of nine ways to evaluate Bayesian model evidence. *Water Resour. Res.* 50. <http://dx.doi.org/10.1002/2014WR016062>.
- Shi, L., Yang, J., Zhang, D., Li, H., 2009. Probabilistic collocation method for unconfined flow in heterogeneous media. *J. Hydrol.* 365 (1–2), 4–10. <http://dx.doi.org/10.1016/j.jhydrol.2008.11.012>.
- Shi, X., Ye, M., Curtis, G.P., Miller, G.L., Meyer, P.D., Kohler, M., Yabusaki, S., Wu, J., 2014. Assessment of parametric uncertainty for groundwater reactive transport modeling. *Water Resour. Res.* 50. <http://dx.doi.org/10.1002/2013WR013755>.
- Smolyak, S.A., 1963. Quadrature and interpolation formulas for tensor products of certain classes of functions. *Dokl. Akad. Nauk SSSR* 4, 240–243.
- Sobol', I.M., 1993. Sensitivity analysis for nonlinear mathematical models. *Math. Model. Comput. Exp.* 1 (4), 407–414.
- Sobol', I.M., Tarantola, S., Gatelli, D., Kucherenko, S., Mauntz, W., 2007. Estimating the approximation error when fixing unessential factors in global sensitivity analysis. *Reliab. Eng. Syst. Saf.* 92 (7), 957–960.
- Song, X., Zhang, J., Zhan, C., Xuan, Y., Ye, M., Xu, C., 2015. Global sensitivity analysis in hydrological modeling: review of concepts, methods, theoretical framework, and applications. *J. Hydrol.* 523 (4), 739–757. <http://dx.doi.org/10.1016/j.jhydrol.2015.02.013>.
- Storlie, C.B., Swiler, L.P., Helton, J.C., Sallaberry, C.J., 2009. Implementation and evaluation of nonparametric regression procedures for sensitivity analysis of computationally demanding models. *Reliab. Eng. Syst. Saf.* 94, 1735–1763.
- Sudret, B., 2007. Global sensitivity analysis using polynomial chaos expansion. *Reliab. Eng. Syst. Saf.* 93, 964–979.
- Sun, Y., Petersen, J.N., Clement, T.P., 1999. Analytical solutions for multiple species reactive transport in multiple dimensions. *J. Contam. Hydrol.* 25, 429–440.
- Tartakovsky, D.M., 2013. Assessment and management of risk in subsurface hydrology: a review and perspective. *Adv. Water Resour.* 51, 247–260. <http://dx.doi.org/10.1016/j.advwatres.2012.04.007>.
- Thomas, T.R., Jaiswal, K., Galkate, R., Singh, S., 2009. Development of a rainfall-recharge relationship for a fractured basaltic aquifer in Central India. *Water Resour. Manage* 23 (15), 3101–3119.
- Tsai, F.T.-C., Elshall, A.S., 2013. Hierarchical Bayesian model averaging for hydrostratigraphic modeling: Uncertainty segregation and comparative evaluation. *Water Resour. Res.* 49, 5520–5536. <http://dx.doi.org/10.1002/wrcr.20428>.
- Tsai, F.T.-C., Li, X., 2008. Inverse groundwater modeling for hydraulic conductivity estimation using Bayesian model averaging and variance window. *Water Resour. Res.* 44, W09434. <http://dx.doi.org/10.1029/2007WR006576>.
- van Griensven, A., Meixner, T., Grunwald, S., Bishop, T., Diluzio, M., Srinivasan, R., 2006. A global sensitivity analysis tool for the parameters of multi-variable catchment models. *J. Hydrol.* 324, 10–23.
- van Werkhoven, K., Wagener, T., Reed, P., Tang, Y., 2008. Characterization of watershed model behavior across a hydroclimatic gradient. *Water Resour. Res.* 44, W01429. <http://dx.doi.org/10.1029/2007WR006271>.
- Vrugt, J.A., ter Braak, C.J.F., Clark, M.P., Hyman, J.M., Robinson, B.A., 2008. Treatment of input uncertainty in hydrologic modeling: doing hydrology backward with Markov chain Monte Carlo simulation. *Water Resour. Res.* 44, W00B09. <http://dx.doi.org/10.1029/2007WR006720>.
- Wagener, T., van Werkhoven, K., Reed, P., Tang, Y., 2009. Multiobjective sensitivity analysis to understand the information content in streamflow observations for distributed watershed modeling. *Water Resour. Res.* 45, W02501. <http://dx.doi.org/10.1029/2008WR007347>.
- Winter, C.L., Nychka, D., 2010. Forecasting skill of model averaging. *Stochastic Environ. Res. Risk Assess.* 24, 633–638. <http://dx.doi.org/10.1007/s00477-009-0350-y>.
- Wholing, T., Vrugt, J.A., 2008. Combining multiobjective optimization and Bayesian model averaging to calibrate forecast ensembles of soil hydraulic models. *Water Resour. Res.* 44, W12432. <http://dx.doi.org/10.1029/2008WR007154>.
- Xiu, D., Hesthaven, J., 2005. High-order collocation methods for differential equations with random inputs. *SIAM J. Sci. Comput.* 27 (3), 1118–1139.
- Yang, J., 2011. Convergence and uncertainty analyses in Monte-Carlo based sensitivity analysis. *Environ. Model. Softw.* 26 (4), 444–457.
- Ye, M., Neuman, S.P., Meyer, P.D., 2004. Maximum likelihood Bayesian averaging of spatial variability models in unsaturated fractured tuff. *Water Resour. Res.* 40, W05113. <http://dx.doi.org/10.1029/2003WR002557>.
- Ye, M., Neuman, S.P., Meyer, P.D., Pohlmann, K.F., 2005. Sensitivity analysis and assessment of prior model probabilities in MLBMA with application to unsaturated fractured tuff. *Water Resour. Res.* 41, W12429. <http://dx.doi.org/10.1029/2005WR004260>.
- Ye, M., Meyer, P.D., Neuman, S.P., 2008a. On model selection criteria in multimodel analysis. *Water Resour. Res.* 44, W03428. <http://dx.doi.org/10.1029/2008WR006803>.
- Ye, M., Pohlmann, K.F., Chapman, J.B., 2008b. Expert elicitation of recharge model probabilities for the Death Valley regional flow system. *J. Hydrol.* 354, 102–115.
- Ye, M., Pohlmann, K.F., Chapman, J.B., Pohll, G.M., Reeves, D.M., 2010a. A model-averaging method for assessing groundwater conceptual model uncertainty. *Ground Water*. <http://dx.doi.org/10.1111/j.1745-6584.2009.00633.x>.
- Ye, M., Lu, D., Neuman, S.P., Meyer, P.D., 2010b. Comment on "Inverse groundwater modeling for hydraulic conductivity estimation using Bayesian model averaging and variance window" by Frank T.-C. Tsai and Xiaobao Li. *Water Resour. Res.* 46, W02801. <http://dx.doi.org/10.1029/2009WR008501>.
- Zhang, C., Chu, J., Fu, G., 2013a. Sobol's sensitivity analysis for a distributed hydrological model of Yichun river basin, China. *J. Hydrol.* 480, 58–68.
- Zhang, G., Lu, D., Ye, M., Gunzburger, M., Webster, C., 2013b. An adaptive sparse-grid high-order stochastic collocation method for Bayesian inference in groundwater reactive transport modeling. *Water Resour. Res.* 49, 1–22. <http://dx.doi.org/10.1002/wrcr.20467>.
- Zhao, J., Scheibe, T.D., Mahadevan, R., 2011. Model-based analysis of the role of biological, hydrological and geochemical factors affecting uranium bioremediation. *Biotechnol. Bioeng.* 108 (7), 1537–1548.